Turbulence in the sea ice impacted Southern Ocean and its implications for primary production and carbon export

Isabelle Giddy

Supervised by Professor Sebastiaan Swart, Dr Sarah-Anne Nicholson and Professor Isabelle Ansorge

UNIVERSITY OF CAPE TOWN
IYUNIVESITHI YASEKAPA • UNIVERSITEIT VAN KAAPSTAD

UNIVERSITY OF GOTHENBURG

Dissertation for the degree of Philosophiae Doctor (PhD)

Department of Marine Sciences, University of Gothenburg
&
Department of Oceanography, University of Cape Town

2022

Turbulence in the sea ice impacted Southern Ocean and its implications for primary production and carbon export

ISBN 978-91-8009-769-7 (printed)
ISBN 978-91-8009-770-3 (pdf)

This book was typeset by the author using LaTeX.

Front cover: © Federico & Patti Soriano

Back cover photo: The author. Photo credit: Ornella Atwell

Quote on opposite page: J.M. Coetzee, Age of Iron, 1990

Printed by: Stema Specialtryck AB, Borås, 2022

Keywords: Southern Ocean, sea ice, submesoscale, diapycnal mixing, heat fluxes, primary production, carbon export, gliders.

to the latitudes where albatrosses fly

Contents

Preface

> Here I am sitting on the golden-silver sand of the beach, casuarinas trees murmuring behind me, the reef rumbling to comfort me in the distance, a lagoon turning from turquoise to orange as I look out at what promises to be a magnificent sunset, asking myself how far I am seeing when I look out to sea. [...] if I look down to my left, would I, if I went straight, get to the South Pole?
>
> *Collen, 2005, p. 71*

Many mornings during the writing of this PhD, I went down to the beach and gazed south towards the horizon over the rippling swell. Beyond sight, expands the Southern Ocean. The story of western discovery of the Southern Ocean begins on the 13^{th} July 1772, when Captain James Cook's ships, Adventure and Resolution, sailed from Portsmouth, England, on his second voyage to search for the fabled southern continent, Tierra Australis Incognito. Upon his return, he logged an abundance of fur seals and whales, opening the doors for their exploitation further south (*Hofman*, 2017). Indeed, the Weddell Sea, takes its name from the sealer, James Weddell, who reached the southernmost latitude at the time in the 1820's (pictured in the image below).

In the early 1900's, Antarctica and the Southern Ocean caught the imagination of explorers, leading to a resurgence of expeditions. In the midst of sea ice in the eastern Weddell Sea is where the recently discovered "Endurance" of Shackleton was engulfed, now sitting on the seafloor, sailing through time. A memory of a tale of courage, strength and hope.

Figure 1: To James Weddell, Esqr R.N... the brig Jane and cutter Beaufoy on 20^{th} February 1823, bearing up in $74°15'$ (Being the highest Southern Latitude ever reached). Hand-coloured. National Maritime Museum, Greenwich, London.

The Southern Ocean is the only ocean around which waters circulate unbounded by landmasses. It is this feature that creates the conditions in which the Southern Ocean plays a central role in regulating the global climate system. Some 30 million years ago the circum-Antartic oceanic belt was formed as the Drake Passage widened, thermally isolating Antarctica and chilling the global climate (*Scher and Martin*, 2006). Without this deep interoceanic link, global climate would be sharply different from what we have today. The Southern Ocean not only promotes

exchange between ocean basins, but it is also the site of major deep-ocean overturning, driven by the sinking of dense upper waters that are formed along the continental margins. Upon reaching great depths and moving northward, this dense water of Antarctic origin cools and ventilates the abyssal layer of the world ocean, affecting oceanic CO_2 storage. It hosts some of the strongest winds, and is known for the roaring forties and furious fifties, making it daunting even for modern maritime traffic and science research vessels. Scientific discovery is especially challenging within the harsh wind, wave and sea ice conditions that dominate the Southern Ocean. Impressive pioneering ship-based oceanographic surveys of the Weddell Sea were carried out since the 1950s; the first through a collaboration between the US and Russia (*Gordon*, 2012), and since the early 2000s, the Good Hope line, running mostly along the Greenwich Meridian and through the Weddell Sea to the Antarctic Continent, has been maintained by multiple national efforts, including South Africa, France and the USA (*Ansorge et al.*, 2005). It was on one of these cruises in 2010 that I first experienced the thrill of scientific discovery aboard the South African vessel, the *RV SA Agulhas* to the almost other-worldly Southern Ocean and Antarctica. It is so remote, that one might wonder why study this ocean so far from human habitation. This was a question I contemplated at the time, given the continuing and pressing structural and socioeconomic injustices in my home country, South Africa, and the need for action in the light of the current climate crisis. Yet, it is here that key climate regulatory processes occur (*Moore et al.*, 2018) where 65% of the world's ocean last make contact with the atmosphere (*De Vries and Primeau*, 2011). It is here that the worlds oceans are replenished of nutrients, maintaining ecosystems and a global fishery (*Sarmiento et al.*, 2004). And so I began to see the link between Africa and Antarctica, and learn of its untold perspectives (*Lavery*, 2019).

In the recent Inter-governmental Panel on Climate Change Special Report on the Ocean and Cryosphere in a Changing Climate (*Meredith et al.*, 2019), the main findings are summarised :

"The polar regions are losing ice, and their oceans are changing rapidly. The consequences of this polar transition extend to the whole planet, and are affecting people in multiple ways"

Building understanding of the processes that occur in these sensitive regions can improve predictions and inform decision-makers. Bringing focus to this unseen world can further motivate rapid action to avert the climate crisis. The innovation of autonomous underwater vehicles (e.g. gliders) has opened the door to low-carbon, sustained, high spatio-temporal resolution observations of the ocean (*Rudnick*, 2016). Pertinently for the remote regions such as the seasonally ice covered Southern Ocean, gliders enable the novel observation of oceanographic processes that are undersampled in time and space. It is with these platforms that I seek to investigate the role of sea ice on regulating upper ocean properties and biological primary production, with the intention to improve the current interpretation of ocean variability and predictions of future ocean and climate conditions. It is my hope that in this way, the body of work presented in this thesis makes a contribution not only to the advancement of science but also to the greater good.

Scientific environment

The research for this dissertation was completed through a double degree agreement between the University of Gothenburg (GU) with the Polar Gliders research group and the University of Cape Town, through which I was affiliated with the Southern Ocean Carbon and Climate Observatory, CSIR. Being part of both of these research groups hosted many an interesting discussion and created an incredibly supportive environment in which to carry out my research. During my PhD I also undertook a research exchange to the University of East Anglia through the Tyndyll Center for Climate Research. A combination of courses and summer schools enriched my experience and provided inspiration and knowledge that drove much of the analysis presented in this thesis. I began my PhD by participating in the GU course "Observing the Ocean from Macro to Micro scale". In many ways, the ideas in this course motivated my approach to this thesis in considering the importance of interactions across scales in the ocean. The foundations for my understanding of turbulence in the ocean were set in the WHOI GFD summer series lectures on turbulence in a stratified ocean, which I attended as a guest student, together with the Masters course, Introduction to Turbulence in the Ocean and Atmosphere, offered at the University of Bergen. The Fluid Dynamics for Sustainability and the Environment summer school hosted by Ecole Polytechnique forged long lasting friendships and broadened my knowledge. The OceanHackWeek virtual summer school, introduced me to collaborative coding and open-source code for science. Finally, a Time Series Analysis course with Johnathon Lilly, beyond building my intuition for spectral analysis which I had been struggling with for a number of years before, gave me new perspectives to data analysis and the undertaking of scientific enquiry at large. The participation in the SCALE cruise during my PhD was a fantastic training opportunity where I deployed autonomous platforms and countless CTDs. This experience also helped to build my intuition for the region that this dissertation is based upon. SEAmester, the South African at sea learning and teaching cruise, was a wonderful way to meet and forge deep relationships with other South African students and scientists. In addition, I had the opportunity to participate in meetings that also developed my whole person. These included Polar Gliders annual research retreats at Börno, a Time to Think workshop and the Life Skills for Young Scientists (LiSYS) meetings with Johnathan Lilly.

Figure 2: A snow petrel fishing in between open-ocean and sea ice during the SCALE cruise, 2019. Photo Credit: Derek Engelbrecht

Acknowledgements

The making of this thesis has been a community effort. I have thoroughly enjoyed the last four years and I thank everyone that was part of the journey.

Seb and Sarah, your enthusiasm for this work is contagious. Thank you for trusting me to take your ideas forward and dive into my own. It has been really wonderful to work you both, thank you for all the great discussions. Seb, I especially thank you for your blue skies thinking and for giving me the space to grow as an independent researcher. Sarah, thank you for inspiring and encouraging me to explore the fascinating world of turbulent flows. Isabelle, thank you for your mentorship and your support to seek out opportunities. I would also like to thank my collaborators during different parts of my PhD: Andy Thompson, Marcel du Plessis, Sandy Thomalla, Bastien Queste and Ilker Fer; I have learnt so much from each of you. Anna Wåhlin, our brief discussions over the years and your guidance went a long way and I am grateful for your input. Importantly, none of the glider deployments would have been possible without the captain and crew of the *RV SA Agulhas II* for which I am incredibly grateful.

I have been lucky to be part of two research groups throughout my PhD. The Polar Gliders research group, it has been so nice to grow along with you, to share our positive thoughts during Monday morning meetings, and to know that you have my back. To everyone at the Southern Ocean Carbon-Climate Observatory, your inputs have always been valuable. Thank you for creating a space that is so warm and welcoming.

To my family, you have cheered me on at every step of the way, in so many ways. To the cabbage patch crew, you were there from the very beginnings of my venture into Oceanography and make my life joyful. Paulo, you are my anchor and my sail. Thank you for being my biggest support during the tough moments and equally, sharing in the excitement of my discoveries. And, of course, I couldn't have done it without my loyal desk mates during the hours spent at home while writing this thesis, Wizard and Misty.

Isabelle Giddy
Cape Town, May 2022

Funding Statement

This thesis was made possible through the generous support of a number of funding agencies. My time at the University of Cape Town was funded by the Oppenheimer Memorial Trust, NRF-SANAP (SNA170506229906), iAtlantic Horizon 2020 grant (818123), UCT Postgraduate Funding Office, UCT Doctoral Research Scholarship and VC Research Scholarship. My travel and research at the University of Gothenburg was funded through the STINT-NRF Mobility Grant (STNT180910357293). A 2-month research visit to the University of East Anglia was funded by the UCT-UEA Newton Climate Fellowship. The field campaigns and research projects within which this thesis was carried out was funded by the grants of S. Swart: Wallenberg Academy Fellowship (WAF 2015.0186), Swedish Research Council (VR 2019-04400); and the grants of S-A. Nicholson and S. Swart: NRF-SANAP (SNA170522231782, SANAP200324510487).

Abstract

The sea ice impacted Southern Ocean, south of the Antarctic Circumpolar Current, is one of the most important regions on earth for the cycling of carbon and distribution of heat and freshwater around the globe. Here, along-isopycnal upwelling of warm, carbon-rich circumpolar deep water coincides with the annual growth and melt of Antarctic sea ice that represents one of the worlds largest surface water transformations. The air-sea-ice buoyancy exchanges and biological processes that change the surface water properties therefore have global consequences, as they set the properties of downwelling intermediate waters that enter the upper branch of the global thermohaline circulation. The region hosts some of the largest uncertainties in global climate models. The reason for this stems from two sources. Firstly, the spatio-temporal resolution of global climate models is limited by computational constraints such that smaller scale processes need to be parameterized. Secondly, the challenges associated with making observations in or near sea ice and in the harsh and remote conditions of the Southern Ocean means that the region is sparsely sampled, and as such, the parameterizations of the small scale and turbulent terms in global climate models are validated based only on a few *in situ* samples. This thesis concerns the observation and interpretation of (sub)meso- to micro scale turbulence and its implications in the sea ice impacted Southern Ocean. I aimed to understand the 0.01-1 km scale physical and biological processes that drive changes in the properties of the upper ocean following sea ice melt, using groundbreaking sustained high temporal and spatial resolution observations made by gliders. There are three main findings. Firstly, we find that sea ice melt enhances stirring of submesoscale flows (0.1-10 km) and therefore lateral variability in the upper ocean, but simultaneously constrains vertical fluxes between the ocean interior and surface. Secondly, turbulent diapycnal mixing and double diffusive convection (0.1-1 m scales) drive the warming of the subsurface winter water, therefore mediating fluxes between the ocean interior and surface. Finally, phytoplankton respond favourably to larger volume sea ice that enhances winter mixing of nutrients from the deep reservoir and upper ocean stratification in the summer. The preliminary evidence from this study suggests that the resultant higher intensity phytoplankton bloom translates to enhanced short term carbon export but not necessarily long term export. Overall, we show, using observations, that the variability and transport of heat and freshwater flux in the sea ice impacted Southern Ocean is sensitive to sea ice, with downstream impacts on phytoplankton, the biological carbon pump and ultimately the upper cell of the meridional overturning circulation.

Sammanfattning

Den säsongsbetonade havsisen i Södra oceanen är globalt viktig för distributionen av värme, färskvatten, koldioxid och näringsämnen. Bidragande till detta är kombinationen av två speciella fenomen: uppvällning av varmt, koldioxidrikt vatten, och ett ythav som påverkas av stor tillväxt och smätning av havsis . De turbulenta processerna som förmedlar utbyte och blandning av vattenegenskaper mellan det uppvällda djupvattnet och det havsispåverkade ytskiktet bestämmer egenskaperna hos vattnet som kommer in i den globala cirkulationen. Det finns dock stora osäkerheter om vilken roll småskaliga turbulenta processer spelar i globala klimatmodeller på grund av modellernas beräkningsbegränsningar, i kombination med sparsam provtagning i avlägsna och svåra förhållanden som är karakteristiska för havsisregionen i Södra oceanen. Denna avhandling handlar om att observera och förstå turbulens från centimeter- till kilometerskala. Det särskilda syftet är att förstå vad som händer i det övre havet efter att havsis smälter, när det gäller blandning av vattenegenskaper och primärproduktion av alger. Vi uppnår detta med hjälp av undervattensdrönare som kan samla in data i havet med hög upplösning i både rum och tid under långa perioder. Det finns tre huvudsakliga fynd: (1) Vi finner att smältningen av havsis ökar horisontella förändringar i kilometerskala i salthalt och temperatur. Havsissmältandet ökar dock också stabiliteten för det blandade ytskiktet, vilket förhindrar vertikal transport av värme och färskvatten mellan havets inre och ythav i de regioner där havsisen smälter. (2) Blandning av värme i centimeterskala i vintervattnet under ytan driver den säsongsbetonade uppvärmningen av detta lager, vilket förmedlar omvandlingen under ytan av det varma och salta djupvattnet. (3) Algtillväxten ökar i förhållande till mängden havsis som växer, främst på grund av att havsisen växer under vintern och kan driva medbringandet av begränsande näringsämnen och mineraler från djuphavsreservoaren till ythavet.

Outline

This thesis is based on four scientific papers referred to in the text by their roman numerals as listed below. The thesis consists of an introductory part, a synopsis of the observations, an introduction to each paper, and the conclusions followed by the scientific papers.

The papers included in this thesis (**chapter 9**) are:

I: Swart, S., M. du Plessis, A.F. Thompson, L. Biddle, **I. Giddy**, T. Linders, M. Mohrmann, S-A. Nicholson, 2020. Submesoscale Fronts in the Antarctic Marginal Ice Zone and Their Response to Wind Forcing. *Geophysical Research Letters*, **47 (6), e2019GL086649**. https://doi.org/10.1029/2019GL086649

II: **Giddy, I.**, S. Swart, M. du Plessis, A.F. Thompson, S-A Nicholson. (2021). Stirring of Sea-Ice Meltwater Enhances Submesoscale Fronts in the Southern Ocean. *Journal of Geophysical Research: Oceans*, **126(4), e2020JC016814**

III: **Giddy, I.**, I. Fer, S. Swart, S-A Nicholson. (*manuscript*, 2022). Vertical convergence of turbulent and double diffusive heat flux drives warming and erosion of Antarctic Winter Water in summer. *in prep for submission to Journal of Physical Oceanography*

IV: **Giddy, I.**, S-A Nicholson, B. Y. Queste, S. Thomalla, S. Swart. (*in review*, 2022). Sea-ice impacts inter-annual variability in phytoplankton phenology and carbon export in the Weddell Sea. *Geophysical Research Letters*

Paper I presents the first data collected as part of this thesis. In **Paper I**, I assisted with the plotting of Figure 2, and computed the surface density spectra plotted in Figure 3b. I also provided input on the uncertainty introduced to lateral gradient approximations given errors in salinity due to uncorrected thermal inertia of the conductivity cell. In **Paper II**, I formulated the research question, performed the data analysis and led the writing and reviewing of the manuscript. I participated in the piloting of the glider that collected the data for the analysis primarily through developing and maintaining a data visualisation website (`www.roammiz.com`). In **Paper III**, I processed the data, formulated the research question, performed the analysis and wrote the manuscript. In **Paper IV**, I deployed one of the gliders used in the analysis (SG640) and participated in at-sea fieldwork as part of the Southern oCean seAsonaL Experiment (SCALE). I formulated the research questions, carried out the data analysis, and wrote the manuscript.

Other works not included in this thesis:

du Plessis, M.D., Swart, S., Biddle, L.C., **Giddy, I.S.**, Monteiro, P.M.S., Reason, C.J.C., Thompson, A.F. and Nicholson, S.A., The daily resolved Southern Ocean mixed layer: Regional contrasts assessed using glider observations. *Journal of Geophysical Research: Oceans*, **p.e2021JC017760**. https://doi.org/10.1029/2021JC017760

In this paper, I contributed to the interpretation of the analysis pertaining to the marginal ice zone, editing of the manuscript, and response to the reviewers.

Gregor, L., T. Ryan-Keogh, S-A. Nicholson, M. du Plessis, **I. Giddy**, S. Swart. (2019). GliderTools: A python toolbox for processing underwater glider data. *Frontiers in Marine Science*. https://doi.org/10.3389/fmars.2019.00738

In this paper, I contributed to the development of the objective mapping component incorporated into GliderTools.

Giddy, I, S. Thomsen, and co-authors. Ocean Gliders Salinity SOP. `https://oceangliderscommunity.github.io/Salinity_SOP/README.html`

I am leading this SOP together with S. Thomsen, collating ideas from co-authors and contributors and maintaining the gitHub repository.

Chapter 1

Motivation

The Southern Ocean acts as a globally important buffer to climate change through its capacity to absorb excess heat (∼75%, *Frölicher et al.*, 2015) and carbon (∼50% *De Vries et al.*, 2017). However, both heat and carbon uptake estimates are model-dependent and have substantial temporal and spatial biases when compared with observations (*Sallée et al.*, 2013). Large discrepancies between global climate models are particularly evident in the seasonally covered sea ice region of the Southern Ocean, where regional and temporal variability of heat and carbon fluxes are poorly constrained (*Gruber et al.*, 2009; *Roden et al.*, 2016). A major control of these fluxes is associated with mixing in the surface ocean boundary layer and the depth of the mixed layer, which modulates the exchange of ocean properties between the surface and ocean interior. If the processes that drive mixing and the depth of the mixed layer are not resolved or are inadequately parameterized in global climate models, the modelled flux of ocean properties will be incorrect.

Ocean circulation in models are based on the continuum equations of motion for seawater (e.g. Navier-Stokes equations), however, due to computational limitations, present ocean models discretize the continuum equations and parameterize unresolved processes, such as submesoscale, O(0.1-10) km, flows (*Fox-Kemper et al.*, 2019). Moreover, a computer model does not indicate if processes are omitted, it simply resolves an incorrect answer. Therefore, experiments and observations are needed in order to determine model biases and unrepresented processes. The bias in mixed layer depth improves with model resolution, highlighting the contribution of ocean circulation (advection and air-sea fluxes) to deep mixing (*Small et al.*, 2021), and hinting to an important role of submesoscale ageostrophic processes. The seasonally sea ice-covered Southern Ocean is remote and inhospitable; a challenging location for observational oceanography. Because of this, observations are sparse (*Lenton et al.*, 2013; *Swart et al.*, 2019). This means that there is little data to validate and improve ocean models.

Given the rapidly changing atmospheric forcing and circulation in the Southern Ocean (Figure 1.1), as outlined in the IPCC Special report (*Meredith et al.*, 2019) on the Ocean and Cryosphere, and the disproportionate role of the Southern Ocean on the climate system, we can infer that even small inaccuracies in its representation in global climate models can have potentially large implications.

This thesis contributes to the existing and growing body of literature by addressing the mechanisms that impact the transport and redistribution of heat, freshwater and

carbon in the sea ice impacted Southern Ocean at scales of centimeters to kilometers (micro- to (sub)mesoscales) using *in situ* observations by autonomous surface and underwater vehicles. It marks the first time that upper ocean variability in the sea ice impacted Southern Ocean has been observed at spatio-temporal resolutions which resolve the evolution of physical and biological phenomena at the submesoscale and below.

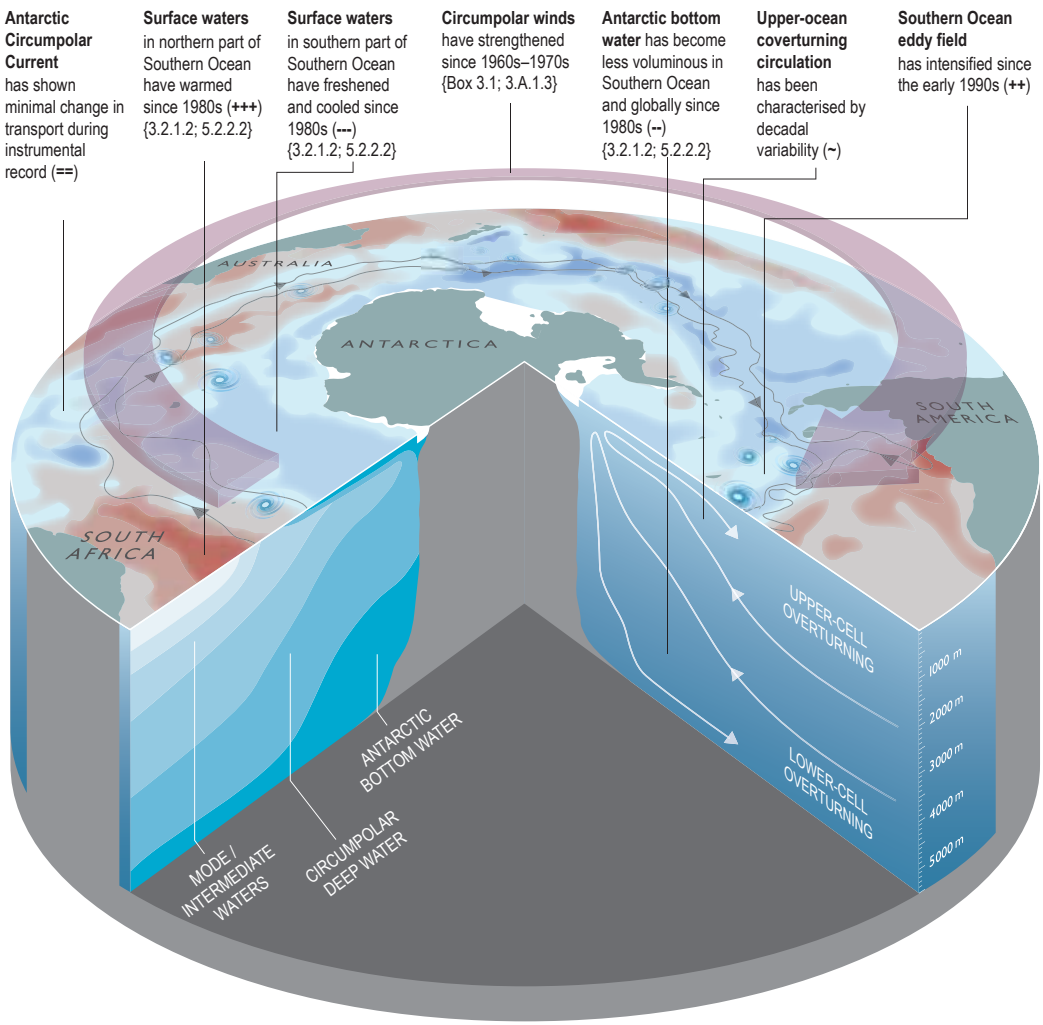

Figure 1.1: The major Southern Ocean changes assessed in the IPCC Special Report on the Ocean and Cryosphere (Meredith et al., 2019). The circumpolar circulation together with the prevailing westerly winds are highlighted. We draw attention to the major water masses and their link to the overturning circulation. Recent (since the 1980s) surface ocean trends (cooling and freshening of the subpolar ocean, warming in the northern Southern Ocean) are illustrated with the blue and red coloring around Antarctica.

Chapter 2

Background

2.1 The importance of Antarctic sea ice

The subpolar region of the Southern Ocean, south of the Polar Front, influences the global climate system over a broad range of space and timescales through the intersection of sea ice formation and melt with sites of deep-water formation and ventilation. Annually, sea ice cover ranges from $\sim$19 million km^2 in austral winter to $\sim$3-4 million km^2 in austral summer (*Parkinson*, 2019). Its distribution and extent is dynamic, with high inter-annual and regional variability and is sensitive to a range of air-sea feedback mechanisms (e.g. wind-driven sea ice drift, Atlantic warming; *Eayrs et al.*, 2019; *Holland and Kwok*, 2012; *Li et al.*, 2014). The transformation of the upper ocean by sea ice growth and melt plays a crucial role in modulating the radiative and thermodynamic properties of the ocean surface, the exchanges of heat, gases and momentum between the ocean and atmosphere, the meridional overturning circulation (*Abernathey et al.*, 2016), and ocean productivity (*Arrigo et al.*, 2008) that supports vast phytoplankton blooms, ecologically important krill, whales and seabirds (*Massom and Stammerjohn*, 2010).

Since the beginning of the satellite observation period in 1979, Antarctic sea ice exhibited a slight increasing trend until 2016 when sea ice was first observed to decline. The slight increase in sea ice extent has been linked with cold sea surface temperatures (*Comiso et al.*, 2017), with enhanced westerly winds driving northward sea ice transport and cooling the sea surface (*Haumann et al.*, 2020). The decline in sea ice since 2016 has been linked to a warmer upper ocean as a result of a shift in atmospheric forcing driving enhanced upwelling of deeper warm water (*Meehl et al.*, 2019). Thus, Antarctic sea ice is sensitive to both atmospheric and oceanic variability that changes the distribution of heat in the Southern Ocean.

A significant long-term decline in Antarctic sea ice remains to be observed, but appears in climate models predicting a warmer climate with warmer ocean surface temperatures (*Roach et al.*, 2020). The decline of Antarctic sea ice will likely have widespread ramifications, however, because of the multiple interacting processes across different time and space scales, the climate response remains an area of uncertainty. For example, recently the albedo effect of only three years of observed sea ice decline in the Southern Ocean between 2016-2018 alone, reversed the global sea ice-albedo climate feedback from a cooling trend to a warming trend (*Riihelä et al.*, 2021). This suggests that Antarctic sea ice decline will enhance global warming. In contrast, a

decrease in sea ice cover may result in enhanced net primary productivity in the ocean surface which could offset carbon in the atmosphere (*Barnes*, 2015; *Henson et al.*, 2022; *Tagliabue et al.*, 2021), and mediate warming.

Atmospheric and intrinsic ocean variability influence the annual growth of sea ice through its role in the variability of buoyancy, stratification (*Pellichero et al.*, 2018; *Wilson et al.*, 2019) and lateral gradients (*Biddle and Swart*, 2020) in the upper ocean. Sea ice is central to the modulation of upper ocean turbulence, the extent of surface mixing (mixed layer depths), and the transport of water properties between the surface and ocean-interior thus setting up a tight feedback mechanism between the atmosphere, ice and ocean.

2.2 Circulation in the subpolar Southern Ocean

In considering the role of sea ice in modulating fine-scale (centimeter to kilometer scale) ocean dynamical and the linked biological processes, it is necessary to consider the water masses and general circulation of the Southern Ocean south of the Antarctic Polar Front (Figure 2.1), within which these processes occur.

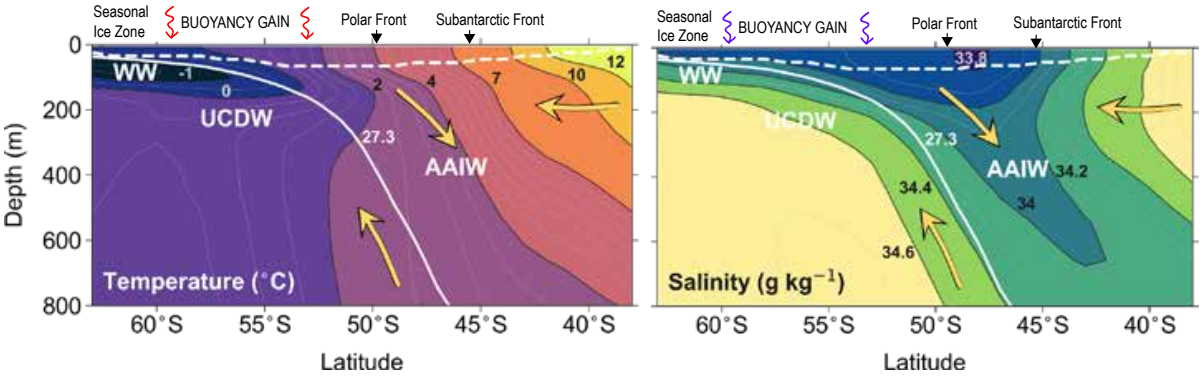

Figure 2.1: Meridional sections of (left) Temperature and (right) Salinity in the Southern Ocean, showing the approximate position and properties of Antarctic winter water (WW), Upper Circumpolar Deep Water (UCDW) and Antarctic Intermediate Water (AAIW), and Southern Ocean fronts. Surface layer buoyancy gain through heat and freshwater flux into the ocean is indicated. Adapted from du Plessis et al. (2022)

The subpolar Southern Ocean is one of the most important regions on earth for the cycling of carbon and distribution of heat and freshwater around the globe (*Abernathey et al.*, 2016; *Hoppema*, 2004; *MacGilchrist et al.*, 2019). It is a region where dense waters return to the surface in nearly adiabatic pathways along tilted density surfaces. The persistent, strong band of westerly winds drives surface divergence which results in upwelling polewards of the zonal surface-wind maximum and downwelling equatorwards of the maximum. When warm, salty, CO_2-rich Upper Circumpolar Deep Water (UCDW) comes into contact with the surface waters and atmosphere exchange of water properties occurs such that its buoyancy increases. Wind-driven Ekman transport advects this water northward, which then subducts as Antarctic Intermediate Water (AAIW), entering the upper limb of the meridional overturning circulation (MOC, *Marshall and Speer*, 2012; *Speer et al.*, 2000, Figure 2.1). The buoyancy gain required

for the transformation of UCDW to AAIW is a topic of relatively recent discussion. Initially, it was understood that the water mass transformation was dependent on the location of upwelling relative to the time-mean air-sea ice buoyancy flux (*Marshall and Speer*, 2012). It has also been argued that buoyancy gain in upwelled UCDW is achieved through the propagation of the surface freshwater via vertical mixing at the base of the mixed layer (*Iudicone et al.*, 2008). Indeed, the buoyancy of the subpolar Southern Ocean is largely determined by the seasonality of sea ice and its associated freshwater fluxes (*Pellichero et al.*, 2017). The seasonal role of sea ice in water mass transformation was suggested by *Abernathey et al.* (2016), where the relative influence of atmospheric, sea ice, and glacial freshwater fluxes, heat fluxes, and upper-ocean mixing in buoyancy transformation within the upper branch of the MOC were assessed. Freshwater input from northwards advected sea ice emerged as a dominant term, emphasising the sensitivity of water mass transformation to changes in winds and wind-driven sea ice transport. These results were confirmed in a similar analysis using observations (*Pellichero et al.*, 2018). The upwelling deep water is preconditioned for transformation by initially becoming colder and fresher via subsurface diapycnal mixing driven by by gravitational instabilities and convection during winter ocean heat loss (*Tamsitt et al.*, 2018). *Evans et al.* (2018a) corroborate this result in showing how the seasonal mixing of winter water (saltier and denser in winter, fresher and warmer in summer) acts as a conduit for the transformation of deep water to intermediate water. They propose cabbeling instabilities (when two water masses mix to form a denser water mass), a process that is linked with brine rejection by sea ice formation, as a primary mechanism driving the mixing of UCDW with the overlying winter water. In addition to these vertical processes, lateral variability in density from heterogeneous ice formation and melt creates the potential for submesoscale instabilities and flows to grow, thereby efficiently transporting water between the subsurface and surface resulting in the rapid restratification of the upper ocean (*Biddle and Swart*, 2020; *Manucharyan and Thompson*, 2017; *Thomas et al.*, 2008). Thus, sea ice mediates the turbulent processes in the upper ocean that can lead to the exchange of properties between the ocean interior-surface and atmosphere. High resolution observations of temperature, salinity and turbulent dissipation are used to progress our understanding of these sea ice mediated turbulent flows and their link to water mass transformation in *Papers II and III*.

2.3 Turbulence in the seasonal ice zone

One of the most important places for ocean turbulence is the ocean surface boundary layer. Because of the direct connection between the surface boundary layer and the upwelled UCDW (Figure 2.1), mixing processes that occur in this layer, such as advection, stirring, turbulent diffusion, and convection, mediate the exchange of heat, freshwater and CO_2 between the atmosphere and ocean interior. The ocean surface boundary layer is characterized by a mixing layer that is formed through active turbulent mixing either by winds or convection, and a mixed layer, representing the mixing that has recently occurred where ocean properties are well mixed and relatively homogeneous with depth.

Looking at the Sentinel1 radar image of the surface ocean (Figure 2.2a), a field of

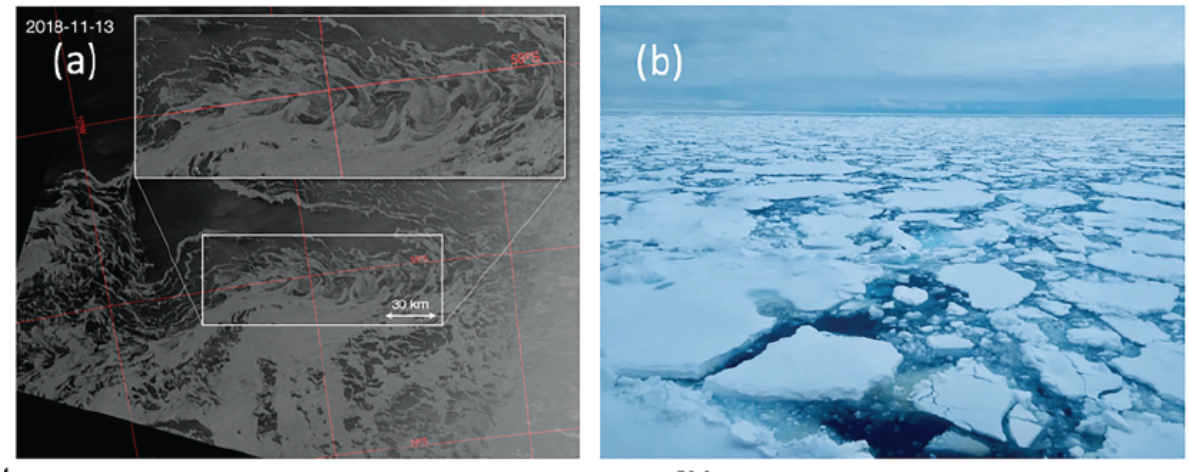

Figure 2.2: (a) Sentinel1 synthetic aperture radar image from 13 November 2018 (1 month prior to robotic deployments) suggesting ocean submesoscale features present at the sea ice margins of O(5-10 km). (b) Photo taken from the RV SA Agulhas II (15 December 2018; 61.07°S, 0.05°E) showing sea ice conditions ∼100 km south of the study location. Image from Swart et al. (2020).

filaments of varying length-scales form patterns in the sea ice, reflecting the underlying fluid motions. This thesis focuses on turbulent processes from the submeso to microscale that act to mediate the properties of the upper ocean following sea ice melt. Before addressing each of these processes and their driving mechanisms, we broadly introduce the scales of turbulent motion in the ocean.

Gradients in the ocean are stirred, strained and sharpened by a range of ocean flows forced by fluxes of momentum, heat and freshwater at the ocean surface (from ocean gyres, mesoscale and submesoscale eddies, internal waves) to small enough scales where 3-dimensional turbulent dissipation and molecular diffusion act to mix ocean properties. This cascade of ocean gradients represent the underlying processes in which energy is transferred across lengthscales via a turbulence cascade until reaching the lengthscale at which dissipation becomes dominant (Kolmogorov lengthscale, *Kolmogorov*, 1941). In the ocean interior, the large scale motions with scales $O(10)$ km or more, are described by balanced sub-inertial quasi-geostrophic dynamics in which there is an inverse cascade of energy (*Charney*, 1971; *Kraichnan*, 1967). At the smallest scales (less than $O(10)$ m), shear instabilities, convection and breaking internal waves produce isotropic 3-dimensional turbulence that effectively and irreversibly mixes ocean property gradients in the ocean. Submesoscale flows with characteristic scales of $O(0.1\text{-}10)$ km occupy the intermediate space and timescales between geostrophic mesoscale eddies and the fully 3-dimensional turbulence and are a key intermediary in the cascade of kinetic energy from mesoscales towards microscales (*McWilliams*, 2016). The irreversible mixing across isopycnals of water properties is the result of dissipation at centimeter scales. It is this mixing that ultimately results in the transfer of heat, salt, gases and nutrients between water masses. Thus, while it is large scale processes that drive the transport of ocean properties and the rate of dissipation; through their mediation of ocean mixing, these small-scale processes are strongly linked to large scale dynamics.

2.3.1 Submesoscale macro-turbulence

Submesoscale ocean dynamics and instabilities can play a critical role in setting the oceans surface boundary layer thickness and associated density stratification. Submesoscale instabilities contribute to lateral stirring and tracer dispersal. In the ocean, they have horizontal scales of O(0.1 - 10 km) and timescales of hours to weeks (*McWilliams*, 2016; *Thomas et al.*, 2008). At these scales, the flows are less constrained by Earth's rotation than mesoscale dynamics but more constrained than more 3-dimensional structures. Dynamically, submesoscale processes are characterised by order one Rossby and Richardson numbers (*Thomas et al.*, 2008). The Rossby number, arising from the relative scaling of the inertial and Coriolis terms in the equations of motion, is defined as $R_o = U/fL$, where U is the characteristic horizontal velocity scale, f is the local Coriolis frequency and L is the characteristic horizontal length scale. The Richardson number describes the ratio of stratification to vertical shear, $Ri = N^2/S^2$.

Upper ocean turbulence in submesoscale fronts, eddies and filaments can be associated with strong vertical velocities, transporting water (and its properties; heat, inorganic and organic carbon, and nutrients) between the ocean interior and surface (*Freilich and Mahadevan*, 2021; *Lévy et al.*, 2018; *Su et al.*, 2018). Mixed Layer Eddies, a class of submesoscale flows (*Fox-Kemper et al.*, 2008), arise from baroclinic mixed-layer instabilities and, given sufficient potential energy (i.e. deep mixed layers and strong lateral gradients), can rapidly restratify the upper ocean (*Boccaletti et al.*, 2007; *Mahadevan et al.*, 2012). Winds that blow over submesoscale fronts advect density such that either water column stratification (via isopycnal slumping) is enhanced or, conversely, turbulent overturns at the front are energized (through shear production of turbulence), maintaining the frontal structure and delaying isopycnal slumping and restratification (e.g. *D'Asaro et al.*, 2011; *du Plessis et al.*, 2019). Submesoscale flows further act to advect and redistribute ocean properties including phytoplankton communities (*Lévy et al.*, 2018), and sea ice (*Manucharyan and Thompson*, 2017). The interaction of Mixed Layer Eddies with mechanical wind forcing is illustrated in Figure 2.3. While lighter water will tend to slump over heavier water, resulting in eddy overturning, winds that are oriented down-current will advect water to the left in the Southern Hemisphere, pushing heavier water over lighter water. This introduces instabilities that maintain the front, and arrest restratification by Mixed Layer Eddies.

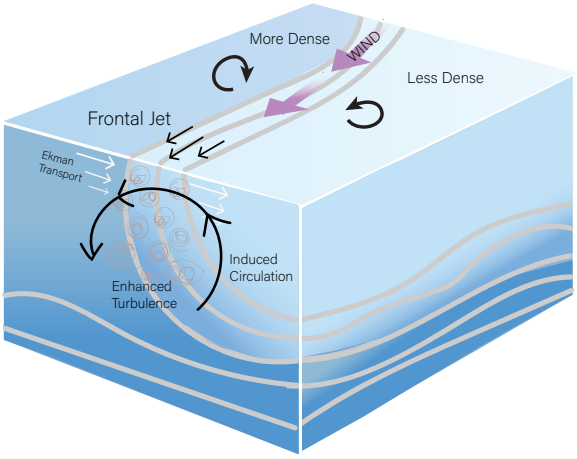

Figure 2.3: Schematic of the flow induced by submesoscale Mixed Layer Eddies and Ekman Buoyancy Flux when the winds are down-front in the Southern Hemisphere, adapted from Mahadevan (2016).

At the edge of the sea ice extent and in the regions of active sea ice melt, heterogeneous ice melt and ice formation introduce lateral density gradients that provide energy for submesoscale instabilities and mixed layer overturns (e.g. *Manucharyan and Thompson*, 2017). While there is evidence of submesoscale features in the seasonal ice

zone year round (*Biddle and Swart*, 2020), their impact on upper ocean stratification and water mass transport is an area of active research. The role of submesoscale flows in the mixed layer of the ice-impacted Southern Ocean is addressed in *Paper I and II*.

2.3.2 Microscale turbulence

The action of turbulent eddies is to disperse particles by stirring which increases concentration gradients and homogenizes fluid properties through diffusion. These two processes lead to efficient mixing at the molecular scale. Mixing across isopycnals (diapycnal mixing) results in the irreversible transfer of heat, freshwater and tracers, a key process in the exchange of water properties and transformation of water masses. The resulting turbulent-enhanced mixing (eddy diffusivity) can be approximated from the rate of turbulent dissipation following the *Osborn* (1980) model. Under steady state turbulence with no transport, the rate of dissipation of Turbulent Kinetic Energy (TKE) is balanced by shear production and buoyancy flux:

$$\underbrace{\varepsilon}_{\text{Viscous dissipation}} = \underbrace{-\overline{u'w'}\frac{d\overline{U}}{dz}}_{\text{shear production}} - \underbrace{\overline{w'b'}}_{\text{buoyancy production}}, \tag{2.1}$$

where z is the depth, $\overline{U}$ is the mean velocity, and $\overline{u'w'}$ is the Reynolds stress. While shear production will always act to create TKE, buoyancy flux can be either stabilizing or destabilizing. As such, processes which either enhance shear production or induce stabilizing or destabilizing buoyancy fluxes can change the rate of dissipation of TKE and therefore the rate of turbulent mixing and transfer of ocean properties.

In the sea ice impacted Southern Ocean these processes include: 1) deep winter mixing driven by brine rejection (*Evans et al.*, 2018a; *McPhee and Morison*, 2001; *Wilson et al.*, 2019) that induces convection and 2) wind and wave-driven shear production of turbulence which is important year-round (*Belcher et al.*, 2012) and plays a key role in the exchange of nutrients and CO_2 across the pycnocline (*Nicholson et al.*, 2019, 2022). Another source of turbulence by which water properties are exchanged is through double diffusive convection (DDC). DDC occurs as a result of the different molecular diffusivities of heat and salt. When cold, fresh water overlies salty, warm water, if a parcel of water is displaced downwards, for example, it will quickly gain heat, and, when returning through the water column with increased buoyancy, will overshoot its original position. This process leads to oscillatory overturns that grow in amplitude and are observed as layering in the ocean. Evidence of enhanced subsurface mixing that results from DDC has been observed in the Ross Sea in winter (*Bebieva and Speer*, 2019) and in the Weddell Sea (*Muench et al.*, 1990; *Shaw and Stanton*, 2014), with a substantial contribution to upwards heat flux observed at Maud Rise. Nevertheless, a global analysis of DDC suggests that the contribution of DDC to the global energy balance is negligible (*van der Boog et al.*, 2021). This analysis was, however, based on the presence of thermohaline staircases from course resolution data. In *Paper III*, we use high resolution direct observations of dissipation to attribute the oceanic processes driving vertical heat fluxes in the summertime, with particular focus on shear-production of turbulence and double diffusive convection.

2.4 Primary production and carbon export in the seasonal ice zone

Biological activity in the upper ocean takes up CO_2 from the atmosphere and converts it to carbon, making it available as food to support higher trophic levels and bacterial communities. About 10% of this carbon is exported into the deep ocean, maintaining a vertical gradient in dissolved CO_2 and allowing for the ocean to continue to absorb natural and anthropogenic CO_2 via the solubility pump (*Sarmiento and Gruber*, 2006). Without this process, it is estimated that CO_2 levels in the atmosphere would be two-fold higher (*Maier-Reimer et al.*, 1996). The sea ice impacted Southern Ocean supports a unique balance between ocean mixing (supply of nutrients) and stratification (light availability), making it one of the most productive oceans regions (*Ardyna et al.*, 2017; *Arrigo et al.*, 2008). Mixing draws up nutrients, while stratification maintains phytoplankton in favourable light conditions. Primary production in this region supports a diverse food-web dominated by krill, marine birds, seals and whales (*Massom and Stammerjohn*, 2010) and drives the biological carbon pump, through the downward transport of particulate organic carbon from the surface ocean to the interior.

The interplay between limiting nutrients and trace minerals, light and predation regulate net primary production across the Southern Ocean (*Arteaga et al.*, 2020; *Tagliabue et al.*, 2014; *Thomalla et al.*, 2011). The sea ice impacted phytoplankton blooms have the strongest seasonal response to light in the Southern Ocean, through the seasonal cycle of solar irradiance, sea ice cover (limiting light) and sea ice melt (enhancing light available by increased stratification) (*Ardyna et al.*, 2017).

The amount of carbon that is exported to the ocean interior is modulated by both biological and physical processes. Direct transport by the physical injection pump (*Boyd et al.*, 2019), which includes that of submesoscale vertical transport (e.g. *Freilich and Mahadevan*, 2021; *Omand et al.*, 2015; *Siegelman et al.*, 2020) has been observed in regions with high eddy kinetic energy. However, the biological gravitational pump is thought to account for the vast majority of carbon export in the world's oceans (*Henson et al.*, 2019; *Martin et al.*, 1987). The efficiency of this export is regulated by the complex interactions of multiple processes, including particle formation and rates of sinking (aggregation, fragmentation, ballasting, senescence, grazing, viral lysis) and remineralization (microbial activity, chemical dissolution), themselves factors that largely depend on rates of primary production and the community composition. It is in part because of this complexity that there remains high uncertainty in future predictions of carbon export throughout the world's oceans (*Henson et al.*, 2022). Because sea ice impacts the stratification and mixing characteristics of the upper ocean, changes in sea ice will have direct implications to the magnitude, duration and community composition of phytoplankton, which will in turn impact carbon flux to depth. Sinking organic carbon that is remineralized within the circulating Circumpolar Deep Water layer currently accounts for about half of the carbon sink in the Weddell Gyre (*Hoppema*, 2004; *MacGilchrist et al.*, 2019; *Naveira Garabato et al.*, 2017), suggesting that changes in the biological carbon pump here (and likely in other subpolar gyres) can have a disproportionate impact on the global carbon cycle (i.e. the soft carbon component of the carbon cycle is enhanced in this region).

While supporting large phytoplankton blooms during austral summer (Figure 2.4

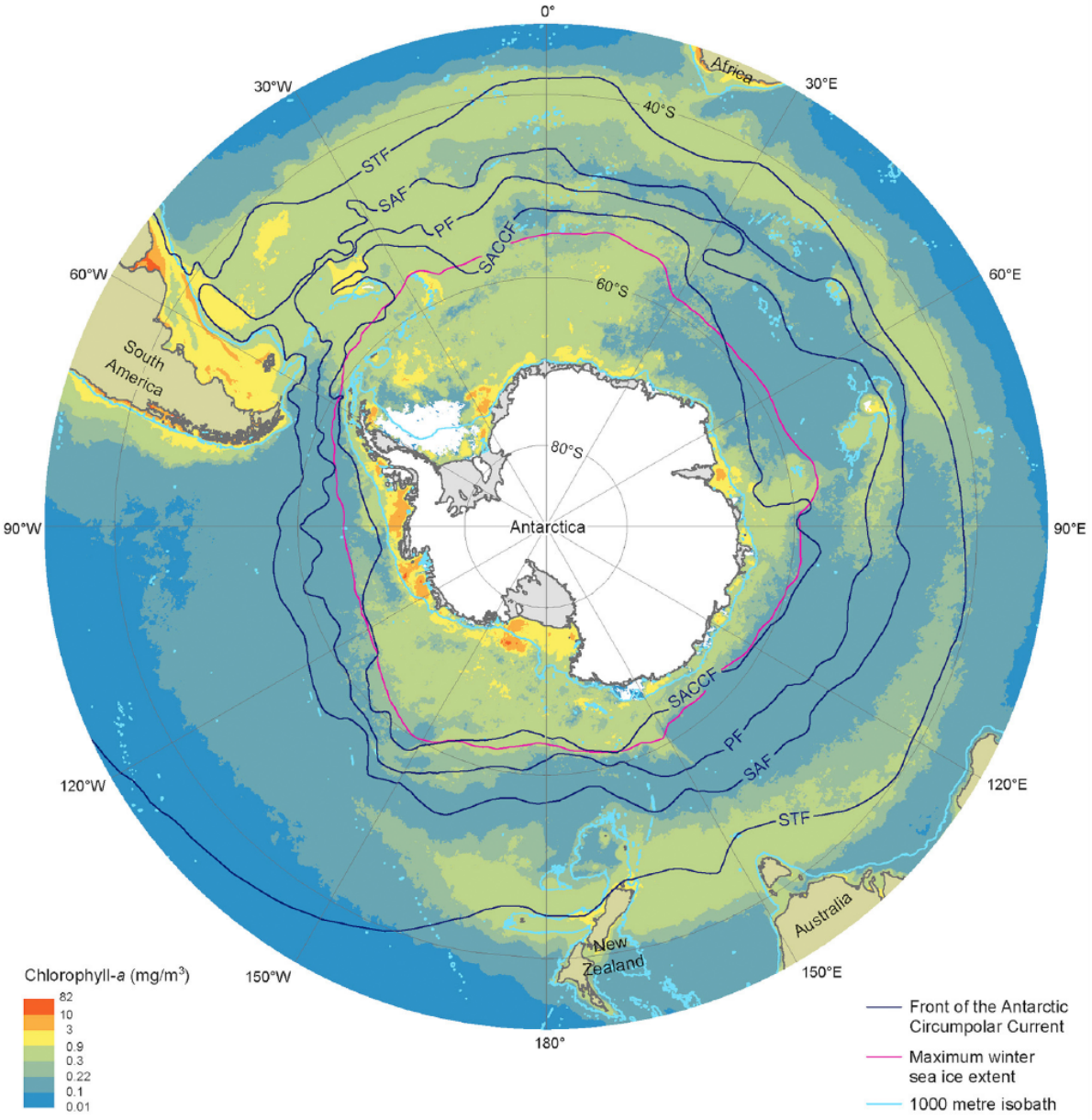

Figure 2.4: Average distribution of Chlorophyll a *in the Southern Ocean. The maximum winter sea ice extent in marked with a red contour line. Image from Deppeler and Davidson (2017)*

.

Deppeler and Davidson, 2017), the sea ice impacted Southern Ocean is sensitive to the changing climate. CMIP6 models predict that both net primary production and carbon export will increase in the Southern Ocean in a warmer climate (*Henson et al.*, 2022; *Tagliabue et al.*, 2021). However, model agreement does not equate to a valid prediction and *in situ* observational validation is important. A recent float based study suggested that net primary production will decrease as a result of either reduced nutrient and mineral availability due to increased stratification (*Arteaga et al.*, 2020), while another study suggests reduced light availability due to enhanced winds may decrease net primary production in the ice-impacted Southern Ocean (*Deppeler and Davidson*, 2017). In *Pinkerton et al.* (2021), depending on the primary production model applied to satellite data, the observed trend in net primary production differed in direction. How any of these changes translate mechanistically to carbon export remains to be quantified as primary production is not necessarily linearly related to carbon export flux (*Henson et al.*, 2019). How phytoplankton respond to the changes in the upper ocean that result from variations in sea ice formation and melt, and how this translates to short and long term carbon storage, is considered through an empirical analysis in *Paper IV*.

Chapter 3

Objectives

The overarching aim of this thesis is to advance the understanding of upper ocean turbulence in the sea ice impacted Southern Ocean using novel, high-resolution observations. The thesis is comprised of four scientific papers that address three distinct topics, each with its own series of research questions. The first three papers focus on mixing processes that modify the properties of water in the upper ocean. The fourth paper assesses the impact of sea ice and associated mixing processes on primary production and carbon export.

1. Submesoscale flows in the sea ice impacted Southern Ocean

    - How does sea ice melt impact upper ocean stratification?
    - Does sea ice melt enhance submesoscale instabilities?
    - Do submesoscale mixed layer fronts vary seasonally?

    Paper I presents the first direct observations of submesoscale lateral gradients in the ice-impacted Southern Ocean using twinned surface and subsurface autonomous platforms. *Paper II* uses three months of glider observations that was deployed directly following sea ice melt, to quantify the length scales and strength of submesoscale fronts in the mixed layer and their seasonal progression.

2. Diapycnal mixing in the sea ice impacted Southern Ocean under stable buoyancy forcing

    - What are the characteristics of turbulent dissipation in the ice-impacted Southern Ocean during summer?
    - What are the drivers of surface and subsurface mixing in the ice-impacted Southern Ocean?
    - Do diapycnal fluxes of heat contribute substantially to the seasonal erosion of the subsurface Antarctic winter water layer?

    Paper III uses measurements of microstructure together with glider observations of temperature and salinity that were made during austral summer to investigate the dominant drivers, characterise turbulent dissipation and quantify the contribution to diapycnal mixing to heat fluxes across the winter water layer.

3. Primary Production and Carbon Export in the Weddell Sea

    - To what extent does sea ice drive phytoplankton bloom amplitude and duration in the Weddell Sea?
    - Can bloom amplitude predict carbon export?

    Paper IV addresses these questions using a combination of satellite observations, biogeochemical Argo floats and gliders observations. The Weddell Sea is a focus region because primary production and carbon export is spatially heterogeneous, warranting a case-study approach.

Chapter 4

Observations

4.1 Overview of the Field Campaigns

In situ oceanographic observations form the keystone datasets used in this thesis. Novel, high resolution observations of the seasonal ice zone are collected through two projects: 1) The Robotic Observations and Modeling of the Marginal Ice Zone (ROAM-MIZ) project (2018-2022) and 2) the SOSCEx-STORM experiment (Figure 4.1a) that involve field campaigns set at the northern reach of the Antarctic Marginal Ice Zone (defined broadly as the transition zone from pack ice to open water) and south of the Antarctic Circumpolar Current. Measurements were carried out between 2018-2020. This comprised of one Sailbuoy deployment (*Paper I*) and three glider deployments: two Seagliders (*Paper I, II, IV*) and one Slocum (*Paper III*). The Slocum was fitted with a turbulence instrument package MicroRider-1000LP (MR). The distribution of each of the gliders sampling patterns is shown in Figure 4.1b,c,d, with sampling concentrated at 60°S; 0°E. The region that the gliders sampled was covered with sea ice during the winter (Figure 4.1a); however the gliders were intentionally deployed directly following the melt of sea ice (e.g. in 2018 SG643 was deployed 4 days after the local melt of sea ice), which occurred towards the end of November and beginning of December, to capture the sea ice driven modifications to the surface oceans and its evolution through summer (Figure 4.1e). During the measurement period, the mean heat flux into the ocean was positive in the daytime (stabilizing conditions), which gradually decreased towards the end of each deployment during the onset of austral autumn. Table 4.1 summarises the respective autonomous platform deployments. In addition to these observations a number of openly available datasets were used (satellite observations, reanalysis and floats) and are detailed in the sections that follow.

Table 4.1: List of autonomous platforms used in the thesis, detailing respective deployment and retrieval dates, sampling pattern and the paper that the data is used in. All deployments were centered at 0°E; 60°S.

name	deployed	retrieved	days	sampling pattern	paper
Sailbuoy	15 Dec 2018	1 Mar 2019	90	mesoscale transects	I
SG643	14 Dec 2018	26 Mar 2019	102	submesoscale bowtie	II, IV
SG640	20 Oct 2019	18 Feb 2020	125	mesoscale transects	IV
Slocum	16 Dec 2019	18 Feb 2020	64	submesoscale bowtie	III

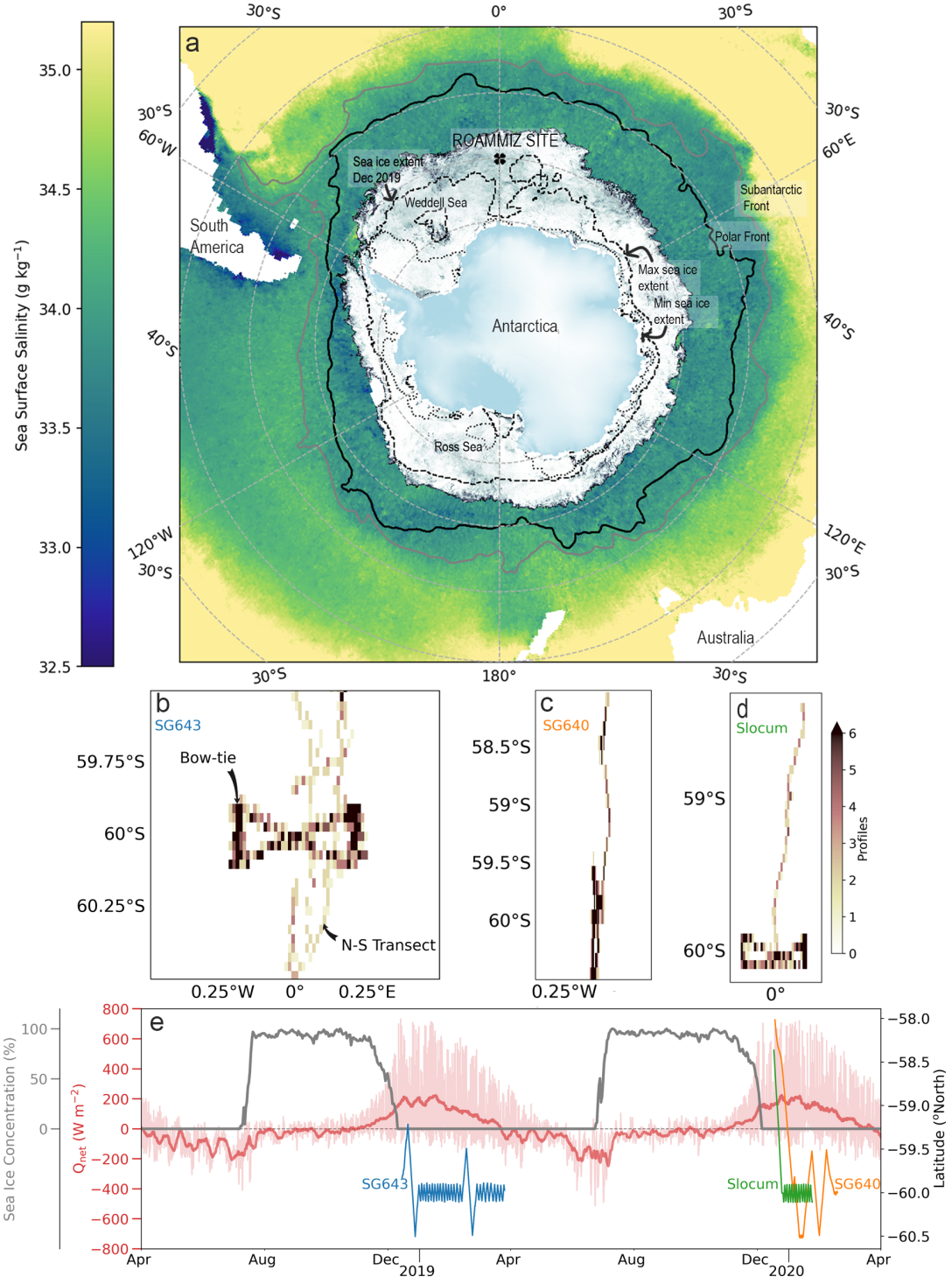

Figure 4.1: Overview of the study region and glider sampling strategy. a) Map of the study region showing the maximum (sea ice colormap) and minimum (dotted line) extents of sea ice and the extent of sea ice at the time of glider deployment (dashed line) in the 2019-2020 annual cycle; the mean location of the Antarctic Polar Front (blue contour) and the Subantarctic Front (grey contour); the ROAMMIZ study site at 60°S; 0°E is marked with an X. The colormap is the average Sea Surface Salinity (SSS) in December 2019 (ESA SSS Climate Change Initiative). Sampling distributions and location of b) SG643, c) SG640 and d) the Slocum glider. e) Time series of sea ice concentration (grey line, Spreen et al., 2008) and net heat flux (red line, ECMWF ERA5) at 60°S; 0°E, together with the latitudinal transects completed by gliders SG643 (blue), Slocum (green) and SG640 (orange).

4.2 Autonomous platforms

4.2.1 Sailbuoy

Sailbuoys are wind propelled with solar panels powering the scientific sensors and navigation systems, allowing them to remain at sea for many months. From 15 December 2018 to 1 March 2019, the Sailbuoy maintained a north-south transect of ∼100 km during which time surface sea water salinity and temperature were measured at 0.5 m depth. Simultaneously, wind speed, wind gust and direction, barometric pressure and air temperature were measured at 0.7 m above sea level. In this thesis (*Paper I*), we focus on the surface measurements of sea water temperature and salinity, and the wind observations.

4.2.2 Gliders

Underwater gliders are a class of autonomous underwater vehicles (AUVs) that profile vertically through the water column by changing their buoyancy and achieve horizontal motion through lift provided by wings. In combination, this results in a characteristic "sawtooth" profiling pattern illustrated in Figure 4.2c. The potential for instruments, such as gliders, in spear-heading future oceanographic observations was imagined in a narrative piece by Henry Stommel (*Stommel*, 1989), where he presents a future scenario of oceanographic observations in which the world's oceans are patrolled by gliders, collecting thousands of ocean profiles a year and likened to the satellite coverage of the ocean surface. While this has not yet come to be, gliders are used extensively in oceanographic research, extending the reach of research vessels in space and time. Gliders can perform sustained, autonomous sampling of the upper 1 km of the ocean. The ability to direct the movement of the glider separates gliders from profiling floats (such as Argo floats) and further allows for the design of unique observational experiments. The high spatio-temporal resolution (2-4 hour; 0.3-4 km; 1 m in the vertical) measurements by gliders build the basis observations for this thesis. Underwater gliders are especially effective for making high resolution observations over longer time periods (weeks - months) because they propel themselves using buoyancy changes and therefore have efficient battery consumption. Their active navigation allows for profiling across currents and fronts in contrast to profiling floats. They allow cross-front measurements to help resolve lateral gradients, while also profiling with depth. In this work the gliders are either piloted to complete "submesoscale bowties" (∼20 km) or "mesoscale transects" (∼100 km) (Figure 4.1). The addition of mesoscale transects, allowed us to evaluate the larger scale ocean gradients within which the submesoscale flows were active. The 'bowtie' pattern is selected in order to build statistically robust sampling of the fronts at the submesoscale. Given that the gliders do not perfectly sample the front perpendicularly can result in a bias, which results in underestimating the lateral gradients from which submesoscale parameterizations are approximated (*Thompson et al.*, 2016).

Seagliders

Two Seagliders (Figure 4.2a) were deployed in consecutive years, austral summer 2018-2019 and 2019-2020 from the *RV SA Agulhas II*. The gliders (SG643 and SG640) sampled temperature, conductivity (salinity), dissolved oxygen, 470 and 700 nm optical backscatter, chlorophyll *a* fluorescence, and Photosynthetically Active Radiation (PAR; only SG643) nominally

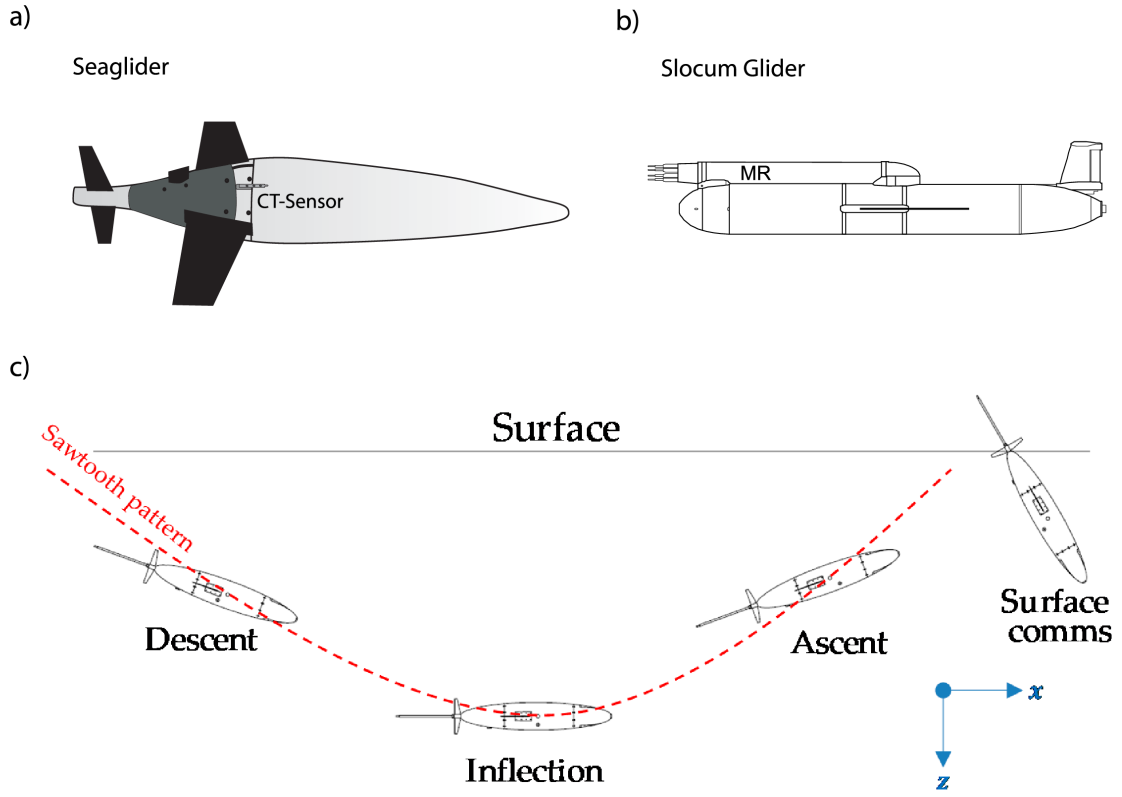

Figure 4.2: Schematics of the two gliders used in this thesis a) Seaglider with the CT sensor labelled and b) Slocum glider with mounted microrider (Fer et al., 2014). c) Typical "sawtooth" glide profile through the water (Orozco-Muñiz et al., 2020).

at 0.2 Hz resulting in a vertical resolution of 0.2-1.5 m in the upper 400 m.

In *Paper II*, SG643 was linearly gridded to 1-km horizontal resolution and 1-m vertical resolution, while in *Paper IV*, both SG643 and SG640 were gridded by profile in the horizontal and binned to 1-m resolution in the vertical. The different choices in gridding pertain to the different research questions that are addressed in each of these papers.

Slocum

A 1000-m-rated Teledyne Webb Research (TWR) Slocum electric glider, G2 (Figure 4.2b), was deployed from the *RV SA Agulhas II* at 58°S, 0°E on the 17^{th} December 2019. The glider then transited directly south for 10 days, completing a mesoscale transect ($\sim$224 km), until it reached 60°S on the 25^{th} December (Figure 4.1). Thereafter, the glider completed a bow-tie pattern of shorter submesoscale transects ($\sim$20-60 km) until it was retrieved on the 18^{th} February 2020. The Slocum sampled temperature, conductivity (salinity), dissolved oxygen, 470 and 700 nm optical backscatter and chlorophyll *a* fluorescence. The sampling frequency was 1 Hz, with an average flight speed of 0.3 m s^{-1}, resulting in a vertical resolution of 0.2 m. In addition, the glider was fitted with a neutrally buoyant, lowpower, self-contained turbulence instrument package MicroRider-1000LP (MR), manufactured by Rockland Scientific International. It was equipped with two orthogonal airfoil velocity shear probes (SPM-38), a pressure transducer, a two-axis vibration sensor (a pair of piezo-accelerometers), and a high-accuracy dual-axis inclinometer, from which turbulent dissipation was derived (detailed in *Paper III*). The sampling frequency is 512 Hz on all turbulence channels (vibration, shear) and 64 Hz for the other channels (pitch, roll, and pressure). The Slocum glider data were processed and corrected for thermal inertia using the software kindly provided by Dr. Gerd Krahmann (GEOMAR, Germany). The software included a hydrodynamic model from which the angle of attack and flow rate past the sensor are computed.

All glider data was further prepared for analysis using GliderTools (*Gregor et al.*, 2019).

4.3 Thermal Lag Correction of Salinity

Salinity derived from temperature and conductivity is prone to dynamic errors that are a result of profiling in a dynamic environment characterised by spatial temperature and salinity gradients. While dynamic errors in conductivity and temperature are usually small relative to natural variations, they can compound into large relative errors in derived salinity. This is because, in many regions of the ocean salinity does not vary as much as conductivity and temperature. Dynamic errors can, for example, create false density instability in profiles and false variations in mixed layer depths. This is particularly important in beta oceans (like the subpolar Southern Ocean), where density is set by salinity variations. While there are algorithms that correct for thermal inertia, it is not always possible to correct for all the error (see residual error in Figure 4.3 below). In *Papers I and II* I use density to compute lateral gradients and estimate the activity of submesoscale flows. In these cases, errors due to thermal inertial can propagate to the estimates of lateral density gradients. In *Paper II*, Figure 3, we propose a method to approximate the error by comparing dive-climb and climb-dive plots and then take the root mean square error of the difference from zero.

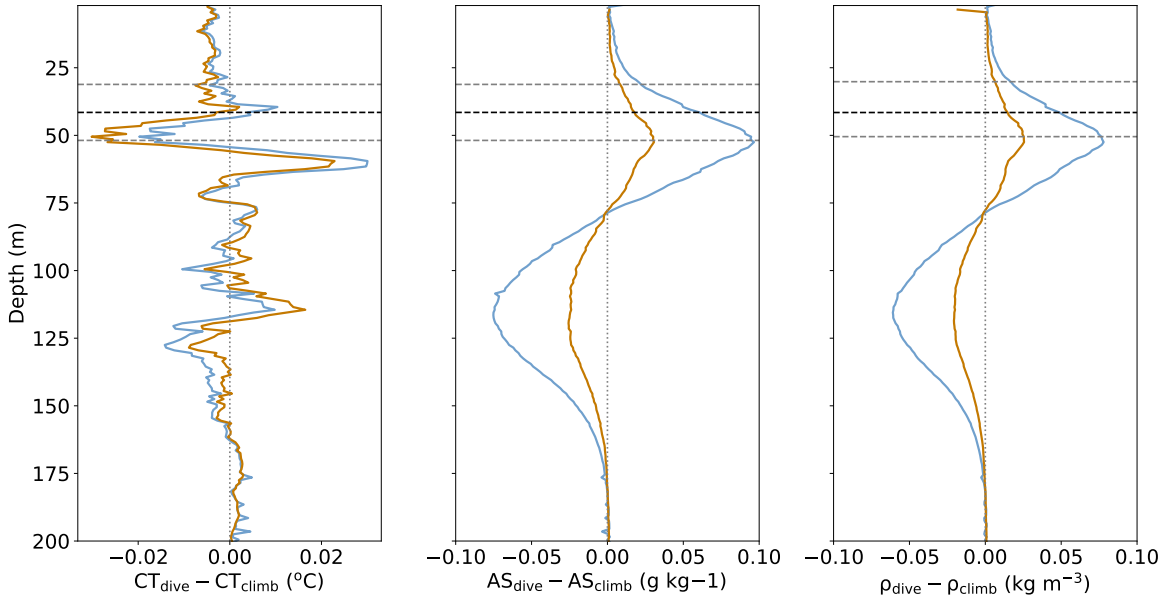

*Figure 4.3: Example of uncorrected (blue) and corrected (orange) Conservative Temperature (CT), Absolute Salinity (AS) and Potential Density (ρ) between consecutive dives and climbs (*Paper II*). The time-averaged mixed layer depth and one standard deviation are shown in the dashed black and grey lines respectively.*

4.4 Microstructure

Direct measurements of microstructure shear variance are used to derive the viscous dissipation rate of turbulent kinetic energy per unit mass, ε (W kg^{-1}). Velocity variance is measured with shear probes that are orthogonal to each other to measure the transverse and vertical components of the along-path shear. Dissipation is then derived from the shear microstructure following *Fer et al.* (2014) using an adaption of the Rockland Scientific ODAS v4.4.04 software. After taking the fast fourier transform (FFT) of the shear (segmented into 30 second intervals, a time scale based on the length of the platform, 1.8 m) and converting it to a wavenumber spectrum using Taylor's frozen field hypothesis, the dissipation rate for each FFT segment is calculated, assuming isotropic turbulence, by integrating the wavenumber spectrum as:

$$\varepsilon_j = \frac{15}{2}\nu\overline{(\frac{\partial u_j}{\partial x})^2} \approx \frac{15}{2}\nu\int_{k_l}^{k_u}\Psi(k)dk, \tag{4.1}$$

where $\frac{\partial u_j}{\partial x}$ is the turbulent scale shear component measured along the glider's along-path coordinate x, j identifies the shear probe number oriented orthogonal to measure the transverse and vertical components of the along-path shear, ν is the kinematic viscosity of seawater, that is a function of the local water temperature, and the overbar denotes averaging. The shear wavenumber spectrum is integrated between k_l, set by the window length and k_u, the minimum in a curve fit to the shear spectrum, that is unaffected by noise. The empirical model for the turbulence spectrum determined by *Nasmyth* (1970) is used to correct for unresolved variance. A number of quality control steps are applied (detailed in Appendix A.1 of *Paper III*), finally taking the average of the quality controlled dissipation estimates from both shear probes. An example of the mean shear wavenumber spectra for dissipation values of 1×10^{-8} W kg^{-1}

measured by each orthogonal shear probe is given in Figure 4.4.

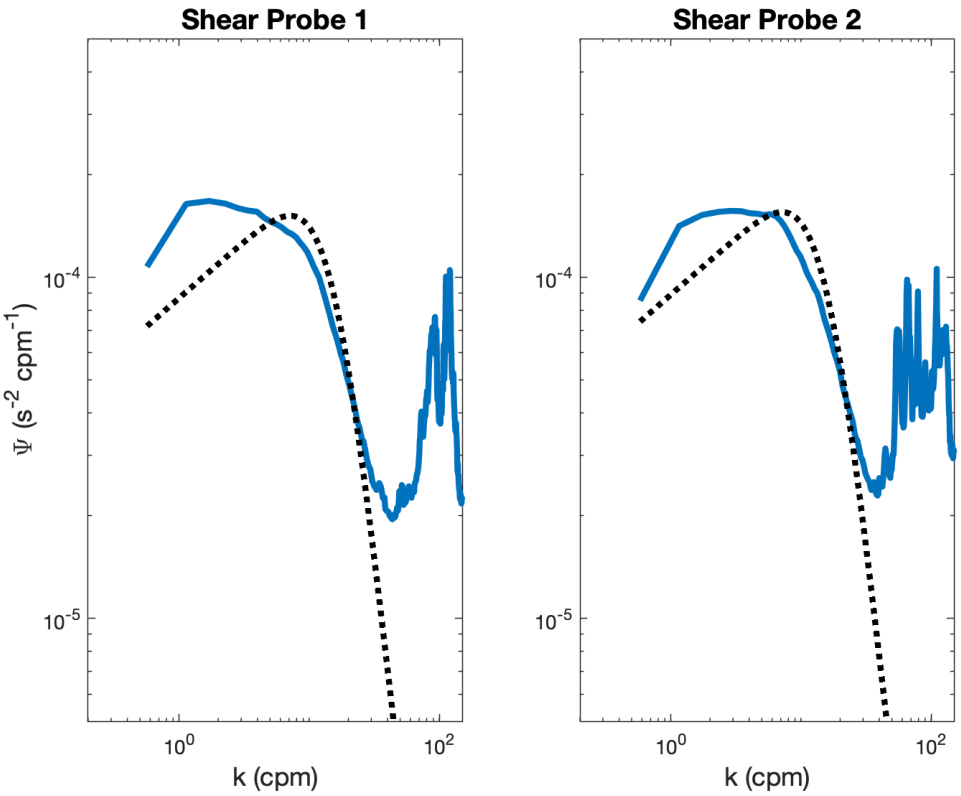

Figure 4.4: Example mean shear spectra measured by each probe for a mean dissipation rate of 1×10^{-8} *W kg*$^{-1}$*. The corresponding Nasmyth spectrum is overlain with the dotted black line.*

4.5 Floats

In this thesis I use Biogeochemical Argo (BGC-Argo) floats, made available by Southern Ocean Carbon and Climate Observations and Modeling (SOCCOM) project. These floats are robotic drifters that move with ocean currents profiling the ocean from the surface to mid-level (2000 m) through adjusting their buoyancy. At depth they drift with the currents, generally programmed to return to the surface once every 10 days. They are equipped with sensors that measure sea water temperature and salinity, and biogeochemical variables, of which I use chlorophyll *a* fluorescence and optical backscatter. In particular, I use two BGC-Argo floats that profiled in proximity to the ROAMMIZ study site from December 2014 to July 2019 (WMO ID: 5094467) and January 2015 to February 2020 (WMO ID: 509397, e.g. Figure 4.5b). For all the float variables only data with a quality control flag of 1 or 2 were used (good or probably good). Potential density was derived from Absolute Salinity and Conservative Temperature (example time-series provided in Figure 4.5a) using the Gibbs Sea Water TEOS-10 Toolbox (*McDougall and Barker*, 2011). Data from these floats is used in *Papers II, III, and IV*.

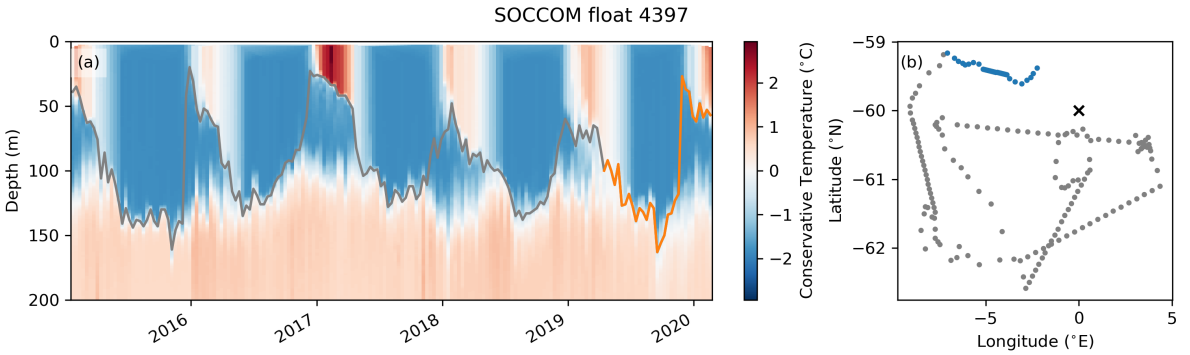

Figure 4.5: (a) Timeseries of Conservative Temperature measured by SOCCOM float 5094397 used in Paper III *to identify the base of the winter water layer. The mixed layer depth is overlain in grey, with the year 2019-2020 in orange. (b) the drift path of the SOCCOM float, with the final year in orange. The study site at 60°S, 0°E is marked.*

4.6 Satellite and Reanalysis Data

Surface heat fluxes, freshwater fluxes (Evaporation - Precipitation), 10 m winds and sea ice concentration are used together with glider data throughout this thesis. In *Paper II*, surface heat and freshwater fluxes and 10 m winds are used in particular for the calculation and interpretation of submesoscale parameterizations. In *Paper III*, these variables are used to interpret the variability of subsurface turbulent heat fluxes. For the calculation of friction velocity (u_*), we use the instantaneous turbulent surface stress product from ERA5, which has similar variability but slightly higher magnitudes than wind stress derived from 10 m winds. In *Paper I*, we show that this product is in good agreement with *in situ* winds observed by the Sailbuoy, providing confidence in the use of ERA5 winds, The shortwave component of the total heat flux is incorporated in the Winter Water temperature budget. Net heat fluxes are used to compute surface buoyancy that is used to interpret the relationship between observed and prediction dissipation as well as the mixing layer depth in *Paper III*. In *Paper IV*, surface heat fluxes and winds are used to interpret phytoplankton bloom phenology. Hourly (*Paper I,II,III*) and six-hourly (*Paper IV*) atmospheric reanalysis fields are obtained from the latest European Centre for Medium-Range Weather Forecasts (ECMWF) climate reanalysis product, ERA5, with a 0.25° x 0.25° resolution (*Hersbach et al.*, 2018).

Sea ice concentration and extent is used to contextualise the results in *Papers II and III*. In particular, sea ice concentration estimates over 20 years are used to investigate phytoplankton bloom phenology and sea ice concentration together with thickness is used to develop a metric for sea ice volume in *Paper IV*. Daily sea ice concentration products OSI-450 (1997-2015) (*OSI-450.*, 2017) and OSI-430-b (2016-2019) (*OSI-430-b*, 2019), distributed by EUMETSAT Ocean and Ice Satellite Application Facility (*Lavergne et al.*, 2019), with a spatial resolution of 25 km. Daily thin sea ice thickness, distributed by the University of Bremen, was extracted for the time period (2011-2020) at 40 km spatial resolution. The product is retrieved from observations of the L-band microwave sensor SMOS (Soil Moisture and Ocean Salinity) (*Huntemann et al.*, 2014). The maximum and minimum sea ice extents in 2019 and 2020 are taken from the Sea Ice Index data product, provided by the National Snow and Ice Data Center.

In *Paper IV*, Chl *a* was extracted at 8-daily resolution from the Ocean Color Climate Change Initiative (OC-CCI) v5.0 product, distributed by the European Space Agency (*Sathyendranath et al.*, 2019). MODIS 8-Daily Mean PAR was extracted from the 8-daily 4 km resolution product from 2002 to 2020. The daily product was used from 2019 to 2020 and

co-located with the glider positions and was in good agreement with glider observed integrated daily PAR.

Chapter 5

Submesoscale flows in the sea ice impacted Southern Ocean

Paper I: Submesoscale Fronts in the Antarctic Marginal Ice Zone and Their Response to Wind Forcing.

Paper I was published in *Geophysical Research Letters* in 2020, with coauthors Sebastiaan Swart, Marcel du Plessis, Andrew Thompson, Louise Biddle, Torsten Linders, Martin Mohrmann and Sarah-Anne Nicholson. This paper uses an autonomous surface vehicle coupled with a glider to observe submesoscale lateral gradients in the sea ice impacted Southern Ocean during austral summer. Special thanks for Martin Mohrmann who deployed the platforms and to the Caltech group under Andy Thompson who piloted SG643.

Paper II: Stirring of Sea-ice Meltwater Enhances Submesoscale Fronts in the Southern Ocean

Paper II was published in the *Journal of Geophysical Research: Oceans* in 2021, with coauthors Sebastiaan Swart, Marcel du Plessis, Andrew Thompson and Sarah-Anne Nicholson. I thank Dhruv Balwada and an anonymous reviewer for their valuable input on the development of this manuscript. This paper combines glider observations with atmospheric reanalysis data to investigate the influence of submesoscale flows on the upper ocean and its interaction with surface boundary layer forcing following the melt of sea ice.

In the following, I contextualise *Papers I and II* within the framework of the thesis and summarize the results. The reader is referred to the full papers in chapter 9.

5.1 Context

At high-latitudes, the first baroclinic Rossby Radius of deformation falls below 10 km (*Chelton et al.*, 1998). This is pertinent to the work that follows as it is a key motivation for observing upper ocean variability with autonomous surface and underwater vehicles. Autonomous surface and underwater vehicles (as introduced in chapter 4.2), sample the ocean at 0.1-4 km horizontal scales, therefore enabling one to resolve the scales at which flows become ageostrophic. Prior to this body of work, evidence for submesoscale flows (refer to the definition in chapter

2.3) within sea ice impacted oceans was demonstrated in the Arctic through theoretical work and numerical simulations (*Horvat et al.*, 2016; *Manucharyan and Thompson*, 2017), as well as in observations (*Brenner et al.*, 2020; *Koenig et al.*, 2020; *Timmermans and Winsor*, 2013; *von Appen et al.*, 2018). In the Southern Ocean, a statistical analysis of seal-tag CTD data (Marine Mammals Exploring the Oceans Pole to Pole, MEOP, *Biddle and Swart*, 2020) indicated submesoscale flows persist through all seasons and within sea ice covered regions. In *Paper I* we show, using high-resolution (horizontal scales of 10-100 m) surface observations, that submesoscale fronts were prevalent in summer (when the Rossby Radius was estimated to be $\sim$2 km) following sea ice melt, suggesting that sea ice melt water fronts can energize submesoscale instabilities. In *Paper II*, we used three months of glider observations to quantify the impact and seasonal evolution of these observed mixed layer submesoscale fronts on upper ocean stability and their potential to mediate vertical fluxes of water properties.

5.2 Summary of the results

Within this work, we address the **first objective of the thesis that considers the impact of submesoscale flows in the seasonal ice zone of the Southern Ocean**. Observations of the upper ocean were undertaken in summer thus, the findings are specific to ice-free stabilizing buoyancy forcing conditions. We observe fine scale lateral gradients (fronts) in the surface mixed layer. Haline fronts exceeding 0.5 g kg^{-1} km^{-1} were observed with a Sailbuoy sampling the ocean at a horizontal resolution of 100-300 m (*Paper I*). Similarly, haline fronts of 0.02 g kg^{-1} km^{-1} were observed within the mixed layer with a glider (sampling at a horizontal resolution of 0.5-4 km) (*Paper II*). These fronts are suggested to be formed by strain resulting from stirring mesoscale sea ice melt fronts. When the larger scale mesoscale gradient in salinity decreases later in the summer season, the submesoscale fronts are also observed to weaken (*Paper II*, Figure 6). The difference in magnitudes of the observed fronts is attributed to the higher sampling resolution of the Sailbuoy compared to the glider, and due to the reduction in lateral gradients with depth (shown in *Paper I*, Figure 4).

In *Paper I* the fronts are observed to respond to wind forcing, with strong winds ($\geq$0.3 N m^{-2}) dispersing lateral gradients. Here we proposed that thermohaline shear dispersion following frontal slumping due to baroclinic instabilities weakened lateral gradients. A tracer dye experiment in the Gulf Stream tracked the dispersion of fronts by winds (*Wenegrat et al.*, 2020), providing a direct observation of this process. The analysis of Ekman Buoyancy Fluxes in *Paper II* further supports the finding that there is a strong response of the upper ocean and lateral density gradients to mechanical forcing by winds in this region. The potential for submesoscale baroclinic instabilities to grow is assessed by estimating the equivalent heat flux (buoyancy input by slumping submesoscale fronts) by Mixed Layer Eddies following (*Fox-Kemper et al.*, 2008). We find a weak contribution by Mixed Layer Eddies (Q_{MLE} = 5 - 20 W m^{-2}). Q_{MLE} is weak as a result of the strong stratification by sea ice melt that maintains shallow mixed layers. As such, while submesoscale fronts are formed by stirring of mesoscale sea ice meltwater fronts, submesoscale vertical fluxes are limited to within the mixed layer. Nevertheless, surface enhanced fronts increase the potential for Ekman-driven cross-frontal flow to modulate the stability of the mixed layer and mixed layer properties (with estimates of Ekman Buoyancy Fluxes varying between 100-1000 W m^{-2}).

Wavenumber spectra are used to describe the horizontal density variance in the mixed layer and analyze the seasonal timescale of active scales of energy variance. The average slope of

the spectra computed from the glider measurements (5 m depth, horizontal resolution of 0.5-4 km) ranges from k=2.1-3.6, and from the Sailbuoy measurements the mean slope is k=-2.4, (0.5 m, horizontal resolution of 100-300 m). The approximated slopes are steeper than surface quasi-geostrophic theory but not as steep as that predicted by interior quasi-geostrophic turbulence theory. Acknowledging the uncertainties involved with these calculations, the results suggest that the surface ocean variance in horizontal density is driven by submesoscale dynamics (with shallower slopes representing energy at small scales). If we assume density spectra as a proxy for Potential Energy, we find that the total Potential Energy in the system decreases towards late summer, indicating that the sea ice meltwater, which is exhausted later in summer, may be related to the change in Potential Energy. The density spectral slopes steepen later in the summer season, in accordance with the idea that there is a decrease in the source of mesoscale stirring by sea ice meltwater. However, we acknowledge that the change in slope may be attributed to noise and errors associated with applying spectral analysis to measurements that are not uniformly spaced. Part could also be attributed to sampling resolution. Furthermore, the scales of submesoscale flows might be expected to decrease during late summer as the ocean becomes more stratified, thus requiring even higher resolution observations.

Finally, a major result of *Paper II* is that the strong stratification, also most likely a result of recently melted *in situ* and advected sea ice, reduces the Potential Energy available for submesoscale associated vertical fluxes. This suggests that the subduction of modified waters by sea ice does not occur in the location of sea ice melt. Subduction 'hotspots' in the Southern Ocean have since been observed further north near the Antarctic Polar Front in regions of higher eddy kinetic energy (*Dove et al.*, 2021). However, we found that entrainment events contribute to substantial heat loss in the mixed layer during summer (*du Plessis et al.*, 2022). The role of diapycnal mixing in driving the vertical exchange of water properties in the sea ice impacted Southern Ocean is addressed in the *Paper III*.

Chapter 6

Diapycnal mixing across Antarctic Winter Water

Paper III: Vertical convergence of turbulent and double diffusive heat flux drives warming and erosion of Antarctic Winter Water in summer

This manuscript is currently being prepared for submission to the Journal of Physical Oceanography and was developed with the support of coauthors Ilker Fer, Sebastiaan Swart, and Sarah-Anne Nicholson. I thank Gerd Krahmann for the additional support in processing the Slocum glider data and Sea Technology Services for the assistance in deploying, piloting and retrieving the glider. In the following, the paper is contextualised and a summary of the results is presented. The reader is referred to the manuscript in Chapter 9 for a full discussion.

6.1 Context

After summertime sea ice melt, the mixed layer of the subpolar Southern Ocean largely experiences stabilizing buoyancy forces (freshwater input from meltwater, either from direct 1-dimensional melt or via advection, and incoming solar radiation; *Paper II*). The resulting enhanced stratification dampens submesoscale vertical fluxes and, in *Paper II*, we posit that the subduction of surface transformed waters does not necessarily occur in the same region as where sea ice melts. In that work, we did not consider the subsurface layer, referred to as "winter water" that is capped between the stratified mixed layer and the warm and saline Upper Circumpolar Deep Water (UCDW) beneath. However, in *Paper III*, we show that the winter water thins and warms over the summer season. This was similarly observed in *du Plessis et al.* (2022) where we note that entrainment of winter water cools the mixed layer. *Evans et al.* (2018a) show that mixing between the winter water layer and UCDW is an important step in the the transformation of the deep water mass, UCDW to intermediate water (Antarctic Intermediate Water, AAIW) that forms the upper branch of the Meridional Overturning Circulation. They suggest that this summer transformation occurs through the input of positive buoyancy (from meltwater and solar radiation). In *Paper III*, we use direct observations of the viscous dissipation rate of turbulent kinetic energy (TKE), hereafter "dissipation", to determine the mixing processes that mediate the exchange of properties between the surface, subsurface and ocean interior.

6.2 Summary of the results

In *Paper III*, we address the **second objective of this thesis that considers diapycnal mixing in the sea ice impacted Southern Ocean**. Using direct measurements of microstructure shear, we characterize the time-averaged levels of dissipation and diffusivity in the subpolar Southern Ocean following sea ice melt. We identify two regions of enhanced mixing: Firstly, in the surface mixing layer, of which 84% of the observed dissipation is explained by wind-driven turbulence. Secondly, at the base of the winter water layer, which we attribute to double diffusive convection (DDC). The enhanced dissipation in the subsurface is the most likely a result of DDC given that the winter water is distinguished as colder, and fresher, than the underlying warmer, and saltier, UCDW. Such profiles are associated with Turner Angles (that provides a metric of the relative contribution of temperature and salinity to the local stability of the water column) between $-\pi/2$ and $-\pi/4$. In addition, we observe temperature staircases (*Kelley*, 1990) that occur as a result of DDC and a band of high spice variance (*Middleton et al.*, 2021). We emphasise that DDC is associated with higher rates of eddy diffusivity (turbulence-enhanced mixing) because, unlike mechanically-driven mixing where a portion of the energy is lost to raising the potential energy of the system, in DDC, all the energy is converted to a buoyancy flux. The observed background mixing is attributed to shear-driven turbulence resulting from the steepening of isopycnals by internal waves.

In *du Plessis et al.* (2022), we assessed the mixed layer temperature budget in the Weddell Sea within the broader context of the Southern Ocean, concluding, in agreement with *Paper II*, that variability within the mixed layer cannot be solely explained by 1-dimensional processes alone. In *Paper III*, we developed a subsurface winter water temperature-tendency budget to determine the contribution of mixing processes to the observed warming and thinning of the layer, considering only 1-dimensional processes in the subsurface winter water layer. We find that the observed temperature is well represented by three components: solar radiation, diapycnal mixing and entrainment. The winter water warming trend is explained by the vertical convergence of turbulent and double-diffusive heat fluxes. Notably, 22% of this winter water warming is due to DDC and excluding the enhanced eddy diffusivity compared to that approximated when mechanically-driven turbulent mixing is assumed would underestimate the warming of the winter water layer and therefore water mass transformation in this region.

Chapter 7

Sea ice impact on primary production and carbon export

Paper IV: Sea ice impacts inter-annual variability in phytoplankton phenology and carbon export in the Weddell Sea

Paper IV is currently under review for publication in *Geophysical Research Letters*, with coauthors Sebastiaan Swart, Bastien Queste, Sandy Thomalla and Sarah-Anne Nicholson. I thank especially Louise Biddle as well as Hannah Rosenthal and Johan Edholm who were all on the polar gliders SCALE team onboard the *RV SA Agulhas II*, when together we deployed SG640, the data from which is used in *Paper IV*. I also thank an anonymous reviewer for their valuable input. Here, I introduce and contextualise the paper, expand on some of the methods applied and summarize the results. I refer the reader to the full paper in Chapter 9.

7.1 Context

In the first three papers of this thesis, we focused on the role of sea ice on mediating observed variability in upper ocean turbulence. Here, we shift focus to the role of sea ice in modulating primary production and carbon export through its impact on upper ocean turbulence.

Phytoplankton form the base of the Southern Ocean biological carbon pump. The carbon produced by primary production is either transferred to higher trophic levels, which sustain the foodweb, or directly fluxed to the deep ocean. Carbon may also enter the deep ocean later in the trophic cascade. Biological carbon export in the subpolar gyres, and especially the Weddell Gyre, substantially contributes to the carbon cycle via lateral transport in the Upper Circumpolar Deep Water (*Hoppema*, 2004; *MacGilchrist et al.*, 2019).

While primary production in the Southern Ocean is on average increasing, the response of phytoplankton in the sea ice impacted Southern Ocean is not certain (*Deppeler and Davidson*, 2017). Phytoplankton biomass (chlorophyll *a*) in the seasonally ice-covered Southern Ocean has, until recently, been largely undersampled because satellite observations are impeded by sea ice and cloud cover (*Thomalla et al.*, 2011). Under ice, Biogeochemical Argo floats have allowed for annual observations of chlorophyll *a* (*Arteaga et al.*, 2020) at $\sim$10-day resolution. However, high resolution, seasonal studies remain sparse. It is known that primary production and carbon export flux are not necessarily proportionally related to each other and display high regionality (*Henson et al.*, 2019), with external interacting factors influencing them both

(*Henson et al.*, 2022; *Pinkerton et al.*, 2021). With this work, we simultaneously analyse the variability in primary production and carbon export at sub-daily resolution in order to observe the link between the two and understand how they respond to sea ice and sea ice-induced turbulence.

7.2 Methods

Paper IV applies glider measurements of both physical (temperature and salinity) and biological (chlorophyll *a* and optical backscatter) variables to simultaneously quantify primary production, carbon export, and water column density at scales of hours to days. These metrics, along with Biogeochemical Argo and satellite observations, were used to reveal the response of phytoplankton to ocean processes associated with sea ice growth and melt. One of the main analyses in *Paper IV* assesses the differences in carbon export and transfer efficiencies between two years of glider observations. Carbon export is defined as the ratio between primary production at the surface and carbon flux at the base of the mixed layer. Transfer efficiency is defined as the ratio of carbon flux at the base of the mixed layer to carbon flux at a deeper depth, which we take as the average depth of the deepest winter mixed layer. In this section, I expand on the methods and uncertainties in estimating carbon export and transfer efficiency. It is well known that there is regional variability in the export and transfer efficiency (*Henson et al.*, 2019), however, temporal variability and long term trends are less certain (*Henson et al.*, 2022). With this analysis, we look at the processes which may cause biological carbon export flux to change.

In the absence of *in situ* incubation experiments, primary production is necessarily modelled. The modeling of primary production has been spear-headed by the satellite optics community (*Behrenfeld et al.*, 2005; *Platt and Sathyendranath*, 1993), but the models have been adapted for underwater profiling floats and gliders (e.g. *Arteaga*, 2021; *Hemsley et al.*, 2015). There are two main approaches to estimating primary production. The first is based on chlorophyll *a*, with growth rate estimated as a function of chl *a* and irradiance, the Platt Model (*Platt and Sathyendranath*, 1993), and the Vertically Generalized Production Model, (VGPM; *Behrenfeld and Falkowski*, 1997). VGPM assumes nitrogen limited primary production, which may not hold in the Southern Ocean. The second approach to modeling primary production is a carbon-based approach that makes predictions on phytoplankton growth rate based on the ratio of chlorophyll *a* to carbon, of which there are two variations: the standard CbPM, (*Behrenfeld et al.*, 2005) and the spectrally-resolved CbPM, (*Westberry et al.*, 2008). The long-term trends in Primary Production observed by satellites result in an increasing trend if VGPM is applied and a decreasing trend if CbPM is applied *Pinkerton et al.* (2021). Here, we compare these models using glider observations (*Paper IV*, Figure S9) and find them, at least for the period of observation, to co-vary even though the magnitudes are different (with VGPM and Platt estimates lower than that of CbPM). Estimates of vertically integrated CbPM, based on glider observations, are slightly higher in magnitude, but comparable to the surface only estimates. This implies that assumptions of vertically homogeneous phytoplankton distribution, at least for our period of observation and this region, are reasonable. Estimates of primary production from the above models when blooms are dominated by deep chlorophyll maxima (*Baldry et al.*, 2020), possibly later in the season under nutrient limiting conditions, may not be as comparable to vertically-resolved glider based estimates.

Similarly, there are several ways by which downward fluxes of carbon can be estimated.

Direct measurements from sediment traps (*Lampitt et al.*, 2008) or indirect estimates. For the latter, there are multiple methods; nutrient uptake (*Moreau et al.*, 2020; *Sanders et al.*, 2005), oxygen utilization (*Jenkins*, 1982; *Kheireddine et al.*, 2020), radioisotopes (*Buesseler*, 1998; *Le Moigne et al.*, 2013), quantifying spikes in optical backscatter profiles (*Briggs et al.*, 2011). Indirect estimate methods were used in this analysis. The range of export flux to 100 m based on the *Briggs et al.* (2011) method that we applied in *Paper IV* was comparable to previous estimates in the same region (*Moreau et al.*, 2020; *van der Loeff et al.*, 2011).

All the above indirect methods of estimating primary production and carbon export contain a degree of uncertainty. Taking this into account, we emphasize the relative differences in primary production and carbon export between the two years in comparison rather than their absolute values.

7.3 Summary of the results

With *Paper IV*, we address the **third objective of this thesis that sets out to assess the impact of sea ice on primary production and carbon export in the Weddell Sea**. We find empirical evidence using 10 years of satellite observations together with Biochemical Argo floats that shows that in parts of the sea ice impacted Southern Ocean (e.g. Weddell Sea, Ross Sea), enhanced winter growth of sea ice drives deeper winter mixing and, therefore, increased vertical fluxes of limiting nutrients which support larger magnitude blooms in the following summer. The two sequential summer seasons of glider data provide preliminary evidence that more intense blooms (higher amplitude) lead to higher carbon export, suggesting a potential positive impact of sea ice volume on the biological carbon pump. However, higher export below 100 m was attenuated more quickly with depth and did not translate to substantially higher export past 170 m, the depth of deepest winter mixing. This suggests that more intense blooms and carbon export events may not lead to enhanced long-term carbon storage. It should be acknowledged that we interpret changes in primary production based on one changing variable: sea ice volume/winter mixed layer depth. However, phytoplankton respond to many interacting factors (e.g. nutrients and trace metal variability, irradiance, grazing and their interactions). But without an *in situ* process-study measuring multiple variables or a model that resolves them, it remains challenging to elucidate the exact driver(s) of the variability observed.

We consider three explanations for the decrease in carbon export with depth. Large cells (notably diatoms with additional ballast; *Tréguer et al.*, 2018), would be expected to sink faster, escaping microbial degradation and hence drive a higher transfer efficiency and lower attenuation rate. Although we did not directly measure community composition, chl a:C_{phyto} ratios have been used to infer changes in community composition, with a higher chl a:C_{phyto} typically indicating a larger proportion of diatoms (*Cetini et al.*, 2015). As such, there were likely more diatoms in the community during the 2019-20 summer season (when high chl a was observed) than during the 2018-19 summer season (when low chl a was observed). Alternatively, the higher chl a:C_{phyto} may also represent a higher ratio of fresh, labile phytoplankton in 2019-20 compared to "older", more refractory particulate matter, in 2018-19. Refractory particulate matter does not remineralize as fast as fresher cells and could explain the observed higher transfer efficiency compared to the following year (*Cavan et al.*, 2018). Changes in density with depth can also influence the sinking rate of particles and therefore the flux attenuation rates. The strongly stratified thermocline that was observed during the 2019-20 summer season might have retained particles within the thermocline, exposing the sinking particulate

matter to a longer period of remineralization in the upper ocean, and thus reducing export to depth. Finally, remineralization rates and flux attenuation may be influenced by bacterial load and grazing (e.g. *Cavan et al.*, 2015). Thus, the faster remineralization rates observed in 2019-20 could be a result of higher grazing pressure within the upper 200 m. In conclusion, an outstanding finding is that the export of carbon cannot be directly explained by physics alone, however more observations are required to confirm the results of this investigation.

Chapter 8

Conclusions and Perspectives

8.1 Summary

Sea ice formation and melt in the Southern Ocean accounts for one of the largest phenomena of surface transformation on the planet. Changing, within an annual cycle, from an area of $\sim$19 million km^2 of sea ice covered ocean in the winter months to one of $\sim$3 million km^2 during the summer months (*Parkinson*, 2019). At the northern extent of the sea ice, warm carbon-rich circumpolar deep water upwells (Figure 2.1), such that processes controlling the transformation of water at the surface in the subpolar Southern Ocean have a disproportionate control on the climate system. It has been shown in model and observational data, that sea ice melt exerts a primary control on the transformation of deep water to intermediate water (*Abernathey et al.*, 2016; *Pellichero et al.*, 2018) and temperature trends in the surface and subsurface layers of the subpolar Southern Ocean (*Haumann et al.*, 2020). However, the scarcity of observations has limited the understanding, in particular, of small-scale processes in modulating upper ocean properties and therefore the exchange of climate important variables: heat and carbon. This background broadly forms the motivation for this thesis.

We have illustrated, through high-resolution observations in the subpolar Southern Ocean, the profound role of sea ice in modulating turbulent processes occurring at scales of kilometers to centimeters. These processes, in turn, mediate the upper ocean physical, chemical and biological properties with local and remote implications.

Directly following the austral-summer melt of sea ice, very cold waters together with large freshwater fluxes set the density characteristics of the upper ocean. Within this seascape, we observe lateral gradients over 0.1-10 km in the surface mixed layer, (*Paper I*), that are likely representative of a mixture of submesoscale Mixed Layer Eddies and filaments as well as fronts formed through stirring mesoscale eddies (*Paper II*). The scale and frequency of these features decreases towards the end of the summer season as does the salinity control on mixed layer density. Incoming solar radiation that warms the upper ocean, together with the stirring of sea ice melt water and the increasing stratification, limits the Potential Energy available for mixed layer instabilities (*Paper II*). But the shallow mixed layer means that upper ocean responds readily to wind forcing. Prevailing winds drive vertical mixing (*Paper III*) and wind-front interactions introduce variability to the stability of the mixed layer (*Paper I, II*). While the mixed layer was characterised by lateral heterogeneity in temperature and salinity, the temperature variability in the underlying winter water was largely explained by 1-dimensional vertical processes alone (*Paper III*). Mixing at the base of the mixed layer is attributed to wind-driven

shear production of turbulence, but is again limited by buoyancy effects that are likely introduced by recent sea ice melt. At the base of the winter water, enhanced turbulent mixing is attributed to double-diffusive convection. The rate of mixing at the base of the mixed layer and the base of the winter water contribute to the rate of heat flux convergence into the subsurface winter water layer, its erosion and thus enabling a pathway for exchange of water properties between the ocean interior and the surface and their associated transformation.

Superimposed onto the dynamical flows of the upper ocean in this region, communities of phytoplankton and the ecosystems that they support are actively responding to changes in the environment. On climate relevant scales, they provide a biological medium through which carbon is transferred from the surface to the ocean interior (via the biological carbon pump). In *Paper IV*, we find empirical evidence, using 10 years of satellite observations together with BGC-Argo floats, that increased sea ice formation in winter drives deeper vertical mixing resulting in the entrainment of limiting nutrients and minerals. This translates to enhanced primary production the following summer season. Two years of glider observations of two contrasting seasonal cycles of primary production show that higher surface primary production leads to higher short term carbon export beneath the mixed layer. However, higher short term export does not necessarily imply higher long term export. We find that the efficiency of carbon transfer to depths deeper than the average winter mixed layer maximum in the year of higher primary production is lower compared to the year that experienced lower rates of primary production. The reasons for this fall into two broad categories that require further research. The first is a physics perspective explanation and the second is a biology perspective explanation. Firstly, greater sea ice formation and thus, deeper winter mixing, increased nutrients in the surface waters and stronger bloom, could also lead to higher stratification during the summer, increasing the retention time of particles in the upper ocean and therefore the attenuation rate with depth. Secondly, differing community compositions associated with the different base conditions of the two blooms observed may result in different remineralization rates.

8.2 Implications

Prior to this work, most observational and modelling studies of upper ocean turbulence in seasonal sea ice zones have been focused in the Arctic Ocean (*Appen et al.*, 2018; *Brenner et al.*, 2020; *Scheifele et al.*, 2021; *Timmermans and Jayne*, 2016; *Timmermans and Winsor*, 2013; *Timmermans et al.*, 2012). While the Arctic Ocean shares some similarities with the Southern Ocean (sea ice presence and high seasonality), the Southern Ocean sea ice zone, in which the sea ice is relatively thin ($\sim$0.5 m) and multi-year ice is uncommon, is unique in its circumpolar extent and the persistent and strong winds maintain a relatively weakly stratified upper ocean. We observed slightly weaker lateral fronts (*Timmermans and Winsor*, 2013) and stronger turbulence (*Scheifele et al.*, 2021) than that observed in Arctic ice-free conditions. While the evidence suggests that submesoscale flows are not driving vertical exchange of water properties in the summertime, the associated eddies are indeed responsible for a lateral component in the mixed layer temperature and salinity budgets, such that the mixed layer budget cannot be predicted by 1-dimensional processes alone (*du Plessis et al.*, 2022). The observation of variable Ekman-driven cross frontal flow has the potential to modulate the stability of the mixed layer. The inclusion of submesoscale flows is therefore a necessary parameterization in coupled-climate models to accurately represent mixed layer heat and freshwater transport.

Turbulent dissipation in the sea ice impacted Southern Ocean is often assumed constant in mixed layer budget studies or not included at all (*du Plessis et al.*, 2022; *Pellichero et al.*, 2017). To a large extent, this assumption is due to the unavailability of direct observations. However, the results of *Paper III* present the first observations of turbulent dissipation in the sea ice impacted Weddell Sea of the Southern Ocean. The observations confirm the sensitivity of the mixed layer to wind forcing that was observed in *Papers I and II*. In *du Plessis et al.* (2022), we highlight that in the sea ice impacted Southern Ocean, vertical entrainment of winter water can cool the mixed layer sufficiently to offset winter entrainment of heat from the underlying Upper Circumpolar Deep Water. The winter water temperature tendency analysis in *Paper III* shows that diapycnal mixing is a key term in driving the seasonal warming of this layer and therefore central to the transformation of UCDW to AAIW. The misrepresentation, therefore, of dissipation rates and turbulent-enhanced mixing (eddy diffusivity) has implications for the upper ocean heat budget and water mass transformation. Furthermore, these findings point to the potential for turbulent-enhanced mixing to increase under increased wind intensity (*Young and Ribal*, 2019). This could accelerate the demise of sea ice through enhanced subsurface warming and winter water erosion.

The transport of sea ice and its 1-dimensional impact on mixed layer buoyancy has been emphasised in the literature as an important regulator of water mass transformation in the high-latitude Southern Ocean (*Abernathey et al.*, 2016; *Pellichero et al.*, 2018). The overarching lines of evidence presented in *Papers I, II and III* point to a key role of sea ice linked submeso-microscale processes in setting upper ocean water properties, water mass transformation, and thereby, the global overturning circulation at the macroscale. These findings add insight into the potential physical mechanisms underlying the conclusions of previous work and will allow for improved interpretation of observed and modelled variability in water mass transformation in this region.

Biological carbon export in the Weddell Sea contributes disproportionately to the global carbon cycle (*Hoppema*, 2004; *MacGilchrist et al.*, 2019). In *Paper IV*, we show that deeper winter mixing supports higher amplitude blooms and high export flux in the Weddell Sea. We link deeper winter mixing with increased sea ice formation. Sea ice is likely to decrease in the future (*Roach et al.*, 2020), expanding the area available for primary production. Together with enhanced nutrient supply from low-latitudes (*Tagliabue et al.*, 2021), this would also lead to increased primary production. However, the trade-off between the stabilising effects of sea ice meltwater and the mixing effects of summer winds (*Fitch and Moore*, 2007) will require further inquiry. In concert, CMIP6 models further predict that export flux in the Southern Ocean will increase under future climate change (Shared Socioeconomic Pathways 5-8.5 *Henson et al.*, 2022). Observations already suggest that primary production is increasing in much of the Southern Ocean, although there is uncertainty in trends between primary production models (*Pinkerton et al.*, 2021). The uncertainty in model predictions stems from the complexity of processes that drive both primary production, carbon export flux and export efficiency. Notably, in *Paper IV*, we find that while increased primary production results in increased export flux beyond the mixed layer, it does not necessarily result in increased export flux beyond the deepest winter mixed layer. That is, we find contrasting signs between export efficiency and transfer efficiency. The available evidence suggests that the main difference between the two blooms is their community composition. This implies differences in particle size, with links to sinking speed, bacterial load, grazers and rates of remineralization.

A number of other factors could also be at play that were not considered (e.g. fragmentation, zooplankton and fish vertical migration, particle stickiness). While this work does not provide conclusive process understanding to the biological carbon pump in the Weddell Sea, the results show that phytoplankton respond to sea ice-driven changes in nutrient and light availability, which has impacts on the transfer efficiency of carbon to depth and therefore carbon sequestration.

8.3 Limitations and future directions

The limitations of various aspects of this work pave the way forward for future work. In the following section, we suggest avenues of research that build upon the findings of this thesis. An overall limitation is the need to simultaneously observe small and large scale processes. An understanding of the mesoscale fields in which the gliders are sampling would provide insight into the scales of interacting processes. These details could be provided by, for example, the upcoming Surface Water and Ocean Topography (SWOT) mission, which will observe changes in sea surface height at high resolution ($\sim$4 km). It would be interesting to link satellite observations to the turbulent processes that we observe with gliders, expanding the reach of these types of analyses.

Spectral Analysis methods on moving platforms

The application of spectral analysis methods in order to assess and analyze the nature and variability of geophysical fluid flow is widely in use (as discussed in section 3.3, *Paper II*). In particular, a number of studies have used horizontal spectra to approximate the presence of submesoscale flows (e.g. *Callies and Ferrari*, 2013; *Jaeger et al.*, 2020; *Timmermans and Winsor*, 2013). In *Papers I and II*, we similarly compute the spectra of the horizontal density. We do this for each transect completed by the Sailbuoy and gliders to compare the observed spectra to theoretical spectra of interior and surface quasi-geostrophic and ageostrophic turbulence (*Blumen*, 1978; *Boyd*, 1992; *Capet et al.*, 2008; *Charney*, 1971). The most robust result was the seasonal reduction in Potential Energy (represented by the integral of the density variance spectra). This was supported by the glider mesoscale transects that showed a decrease in mesoscale gradients later in the summer. The analysis of the slope of the density spectra retains some uncertainty, even though we found a degree of agreement with the predicted slopes (with k ranging between -2 and -4). Spectral methods have three challenges: 1) aliasing due to discrete sampling intervals, 2) spectral blurring, due to the truncation of a continuous process to a finite duration, and 3) variance, due to stochastic variability. I will address each in turn with reference to the glider observations.

Aliasing The internal Rossby radius of deformation, L_r, during the observational period ranged from $\sim$0.5-3 km, depending on the vertical stratification. Submesoscale flows can develop only at scales below L_r. To fully resolve submesoscale flows, it would be required to measure with a horizontal frequency of half the L_r. The glider, however, has a horizontal sampling resolution that ranged from 0.3-4 km, which we interpolated to a uniform grid of 1 km. Hence, it is likely that the effects of aliasing, which introduces increased potential energy that is not physical, contaminating the data. This could be improved by increasing the horizontal resolution of sampling, but would mean that the glider would be limited to dive to shallower depths and thus increasing its power consumption.

Spectral Blurring Spectral blurring occurs as an outcome of sub-sampling a continuous process in the time-domain. This blurring smooths the physical process by a box-car window

resulting in a convolution in the frequency domain which introduces broadband bias (error) at low wavenumbers (high frequencies). These effects cannot be avoided but can be reduced by multiplying the data set with optimised tapering windows (the most common being the Hanning window). A result of tapering is the loss of information at the edges of the time series, thereby increasing variance. Therefore, a short timeseries (with a low number of samples, N) will have larger variance than longer timeseries.

Variance Variance occurs as a result of stochastic variability under the assumption of stationarity. There are two approaches to dealing with variance. The first is to average over multiple orthogonal tapers (referred to as the multi-taper method). The second, is to have multiple samples of the same process (repeat transects). However, by reducing variance, the data is smoothed which increased spectral blurring. The trade-offs between the two approaches need to be balanced. Variance could be reduced in Figure 3b of *Paper I* by averaging over the individual Sailbuoy transects. In *Paper II*, we applied multitaper windows and averaged over the shorter $\sim$20 km transects (*Paper II*, Figure 8). These shorter transects were associated with steeper spectral slopes than the mesoscale transects and theoretical predictions. On reflection, it is likely that the observed variance was artificially reduced through tapering and averaging over timeseries with a low number of samples, resulting in steeper than expected slopes.

In addition to these well known challenges of spectral analysis, we necessarily assume that spatial scales are evolving slower than temporal scales and thus interpret the data as a timeseries (assuming a "frozen field"). This is complicated when considering a moving platform that samples in both space and time at non-equal sampling intervals. The more consistent and surface-only sampling of the Sailbuoy has a lower probability of propagating sampling bias, but nevertheless it is not certain what information is lost on either the Sailbuoy or gliders by this assumption. This could be tested using a model that reproduces the same environment that the autonomous vehicle is sampling in. A model analysis would also inform the optimum sampling intervals required to resolve the submesoscale ocean in this region. A mooring could further provide a valuable comparison in a Eulerian field.

The role of mixing in Southern Ocean warming

The Southern Ocean is warming (*Auger et al.*, 2021). The results of this thesis show that in the sea ice impacted Southern Ocean, strong stratification limits the exchange of heat between the interior and surface ocean at submesoscales (*Paper II*), while wind-driven shear production of turbulence can transport heat from the surface to subsurface (*Paper III*). These results contribute to the growing understanding of the drivers of surface boundary layer turbulence in the Southern Ocean, emphasising the latitudinal variation in dominant processes, also highlighted in the recent regional mixed layer budget analysis by *du Plessis et al.* (2022). Because of uncertainties in mixing estimates at the base of the mixed layer, *du Plessis et al.* (2022) neglected the vertical mixing term in their analysis. *Sallée et al.* (2021) use 20 years of observational evidence to show that stratification is increasing in the summertime globally, while simultaneously mixed layers are deepening. They attribute this to increased wind-driven shear production of turbulence, but do not have estimates of mixing to support the postulation. In *Paper III*, I posit that surface-boundary layer turbulence is driven by winds by applying the Law of the Wall surface scaling. To a good approximation, our assumption holds. In addition, the role of Langmuir turbulence in driving boundary-layer turbulence is known to be important in the Southern Ocean in all seasons and especially in the summertime (*Belcher et al.*, 2012; *Li et al.*, 2019). In our results we find an offset between predicted dissipation and measured dissipation. An offset is also identified in independent estimates of dissipation near the Antarctic Polar Front by *Nicholson et al.* (2022). Given the likely important, and increasingly so, role of

winds and waves in driving upper ocean mixing (*Young and Ribal*, 2019), these findings warrant a re-evaluation of the surface ocean boundary layer, scaling with a Southern Ocean focus, especially since most of the observations have been made under destabilizing buoyancy conditions and in the Northern Hemisphere (*Esters et al.*, 2018; *Li et al.*, 2019).

In *Paper III*, we approximate heat flux from observed dissipation rates using the *Osborn* (1980) model. In this model, we reasonably approximate the mixing efficiency, $\Gamma = 0.2$, for mechanically-driven turbulence (*Gregg et al.*, 2018). However, the mixing efficiency varies depending on the turbulent regime (*Bouffard and Boegman*, 2013) and the assumption of a stratified ocean upon which the approximation relies, does not hold within the mixed boundary layer. In order to improve the estimates of heat flux across this layer, which may be more important for water mass transformation than previously understood (e.g. *Abernathey et al.*, 2016, does not include this as an important factor in water mass transformation), an avenue of future research lies in the use of Large Eddy Simulations to directly determine the mixing efficiency under varying forcing and when submesoscale front-wind interactions are active (e.g. *Whitt and Taylor*, 2017; *Whitt et al.*, 2019). An important result of *Paper III* was the identification of a region preconditioned for strong double diffusive convection (DDC) at the base of the winter water layer. In the case of double diffusion, mixing efficiency is close to 1 (*St. Laurent and Schmitt*, 1999), therefore increasing the rate of eddy diffusivity. Through analysis of the winter water temperature budget, we found a substantial contribution to upgradient vertical heat flux via double diffusion. However, global estimates of diffusivity in the stratified ocean do not take this process into account (mixing efficiency is largely taken to be 0.2, under the assumption of shear-driven stratified turbulence). While *van der Boog et al.* (2021) make an argument for its irrelevance to the global energy budget, their study is based on course-resolution quantification of thermohaline staircases, which is sure to underestimate the prevalence of DDC. Quantifying the contribution of DDC to ocean mixing in the changing subpolar Southern Ocean via new methods (e.g. *Middleton et al.*, 2021) and the incorporation of DDC to mixing parameterizations in ocean models seems imperative.

In the Southern Ocean, including the sea ice impacted Southern Ocean, wind-driven upper ocean mixing is important for the distribution of heat between the ocean interior and surface, as suggested by the results of *Papers II and III*. However, in both these works, our conclusions are based on only one season of observations. Recent developments in dissipation parameterizations allow for the estimation of dissipation from high resolution glider observations of temperature and salinity (*Evans et al.*, 2018b; *Middleton et al.*, 2021). With the growing archive of glider observations in the Southern Ocean, applying these methods to gliders will allow for a statistical and regional analysis of the contribution of winds to heat fluxes and thus the sensitivity of Southern Ocean heat distribution to changes in wind forcing.

Double Diffusive Convection

In their recent global analysis of thermohaline staircases, *van der Boog et al.* (2021), conclude that DDC has a negligible contribution to global energetics. In *Paper III*, we find that DDC is likely an important driver of subsurface heat flux into the winter water, contributing to its seasonal warming. Winter water is a circumpolar feature in the subpolar Southern Ocean and therefore DDC is expected to be spatially widespread. *Evans et al.* (2018a) show that winter water acts as a conduit for the transformation of Upper Circumpolar Deep Water to Antarctic Intermediate Water and therefore in controlling the upper limb of the Meridional Overturning Circulation (MOC). Given that DDC is an important process in setting the properties of winter

water, which directly feeds into AAIW and the upper MOC, DDC is likely more important than currently understood. In *Paper III*, we demonstrate the contribution of DDC heat fluxes in one case study. This contribution could be better constrained if a similar analysis is applied to more sample locations, or perhaps to the Southern Ocean Argo array. Adapting the method proposed by (*Middleton et al.*, 2021) for use with gliders and in regions that are sensitive to the non-linearities of the equation of state, could provide further insights to the contribution of DDC to dissipation rates in the subpolar Southern Ocean. Analyses of water mass transformation rate with DCC, and without DDC, may constrain its role in the ocean overturning circulation.

An ecosystem approach to understanding carbon export

In *Paper IV*, we found preliminary evidence that increased winter mixing induced by sea ice formation supports higher amplitude phytoplankton blooms the following summer. This results in increased short-term carbon export but not necessarily increased long-term carbon export. We suggest a number of possibilities for the disconnect between short-term and long-term carbon export, but are unable to definitively come to a conclusion. The limiting factor in this study is the lack of biological metrics. Simultaneous knowledge of the phytoplankton community composition, zooplankton activity and bacterial and viral load and their interactions would enable more robust conclusions. Observations of these metrics at the same spatio-temporal resolution as the glider observations of chlorophyll *a* and optical backscatter are at the frontier of current observational capabilities. The incorporation of imaging platforms on underwater gliders is under development but are currently limited by payload size and power constraints (*Lopez et al.*, 2015). Acoustic Doppler Profilers are however able to estimate zooplankton biomass (*Powell and Ohman*, 2012), although power consumption limits deployment time. A mooring, which could support cytometers and ADCPs in the region deployed simultaneously with underwater glider could elucidate much of the unknowns in such a study. This would further allow for the deployment of sediment traps (*Trull et al.*, 2001) to provide an independent estimate of carbon export, together with the backscatter spike method (*Briggs et al.*, 2011) that was used in *Paper IV*. Finally, we did not measure trace minerals. We attribute the changes in chlorophyll *a* biomass, primary production and phytoplankton community structure to differing supplies of the trace mineral, Iron, mixed into the surface waters during winter. Whether this is the driving process, whether the rate of primary production is Iron-limited, or perhaps Manganese-limited (*Browning et al.*, 2021) can currently only be constrained with direct experimentation using ship-based studies.

Frontiers of glider observations

Observing the ocean with gliders, which can sample the ocean for many months, has become a key platform in advancing our understanding of small scale ocean processes over sustained periods of time and in challenging conditions. If these observations are to become legacy datasets with which we are able to monitor long term change as imagined by Henry Stommel (*Stommel*, 1989), a community approach to the processing and quality control of essential ocean variables is needed. Dynamical errors in salinity arise partly as a result of thermal-inertia, and can become a substantial source of uncertainty when deriving the mixed layer depth or buoyancy gradients, particularly in oceans where the density is set by salinity and in oceans characterized by large thermal gradients. These should be corrected for as discussed in *Paper II*, but more importantly, community collaboration and agreement in the methods for correction are needed in order for cross-platform comparisons. Such standards are being developed by Ocean Gliders and should continue to advance. For initiatives such as these to

be sustainable, additional recognition of work towards open-source community software and the allocation of funding and time to their continuous development, is required.

8.4 Closing remarks

The interdisciplinary scope of this thesis has advanced our understanding of the role of sea ice in modulating multi-scale turbulent processes and the biological carbon pump in the subpolar Southern Ocean. First, lateral density gradients at submesoscales O(0.1-10) km are active following the melt of sea ice in the subpolar Southern Ocean. While these fronts persist through the austral summer season, they are modified by wind interactions. Second, melt water stirring of submesoscale flows sustains lateral variability in the mixed layer, such that the mixed layer heat fluxes cannot be explained by vertical processes alone. However, melt water simultaneously sustains strong stratification at the base of the mixed layer, such that the subduction of surface transformed waters must occur remotely to where they are formed (*Paper II*). Third, beneath the mixed layer, winter water heat variability is well explained by surface and subsurface vertical processes. Variations in temperature are attributable to entrainment and detrainment while the seasonal summertime warming is attributable to diapycnal mixing from wind driven eddy diffusivity at the base of the mixed layer and double diffusive convection at the base of the winter water layer (*Paper III*). Fourth, primary production responds positively following winters with high sea ice volume (enhancing winter mixing and summer stratification), which may result in increased short term carbon export supporting mesopelagic ecosystems. However, we were not able to link long term carbon export to an intrinsic physical process. We hypothesize that long term carbon export is explained by non-linear biologically forced interactions involving rates of bacterial remineralization and phytoplankton community composition (*Paper IV*). The insights gained motivate for urgent focus on this rapidly changing and climatically important oceanic system, with a plethora of open and exciting questions still to be explored.

> "We have found, over the years, that the payoff in increase of knowledge often is greatest the more unconventional the idea, especially when it conflicts with collective wisdom"
>
> *Henry Stommel, 1989*

Bibliography

Abernathey, R. P., I. Cerovecki, P. R. Holland, E. Newsom, M. Mazloff, and L. D. Talley (2016), Water-mass transformation by sea ice in the upper branch of the Southern Ocean overturning, *Nature Geoscience*, *9*(8), 596–601, doi:10.1038/ngeo2749. 2.1, 2.2, 8.1, 8.2, 8.3

Ansorge, I. J., S. Speich, J. R. E. Lutjeharms, G. J. Goni, C. J. d. W. Rautenbach, P. W. Froneman, M. Rouault, and S. Garzoli (2005), Monitoring the oceanic flow between Africa and Antarctica : report of the first GoodHope cruise : research in action, *South African Journal of Science*, *101*(1), 29–35, doi:10.10520/EJC96351, _eprint: https://journals.co.za-/doi/pdf/10.10520/EJC96351. (document)

Appen, W.-J., C. Wekerle, L. Hehemann, V. Schourup-Kristensen, C. Konrad, and M. Iversen (2018), Observations of a Submesoscale Cyclonic Filament in the Marginal Ice Zone, *Geophys. Res. Lett*, doi:10.1029/2018GL077897. 8.2

Ardyna, M., H. Claustre, J.-B. Sallée, F. D'Ovidio, B. Gentili, G. van Dijken, F. D'Ortenzio, and K. R. Arrigo (2017), Delineating environmental control of phytoplankton biomass and phenology in the Southern Ocean: Phytoplankton Dynamics in the SO, *Geophysical Research Letters*, *44*(10), 5016–5024, doi:10.1002/2016GL072428. 2.4, 2.4

Arrigo, K. R., G. L. van Dijken, and S. Bushinsky (2008), Primary production in the Southern Ocean, 19972006, *Journal of Geophysical Research*, *113*(C8), C08,004, doi:10.1029/2007JC004551. 2.1, 2.4

Arteaga, L. (2021), artlionel/SOCCOM_bgc_float_data_public:v1.0, doi:https://doi.org/10.5281/zenodo.4770029. 7.2

Arteaga, L., E. Boss, M. J. Behrenfeld, T. K. Westberry, and J. L. Sarmiento (2020), Seasonal modulation of phytoplankton biomass in the Southern Ocean, *Nature Communications*, *11*(1), 5364, doi:10.1038/s41467-020-19157-2. 2.4, 7.1

Auger, M., R. Morrow, E. Kestenare, J.-B. Sallée, and R. Cowley (2021), Southern Ocean in-situ temperature trends over 25 years emerge from interannual variability, *Nature Communications*, *12*(1), 514, doi:10.1038/s41467-020-20781-1. 8.3

Baldry, K., P. G. Strutton, N. A. Hill, and P. W. Boyd (2020), Subsurface Chlorophyll-a Maxima in the Southern Ocean, *Frontiers in Marine Science*, *7*, 671, doi:10.3389/fmars.2020.00671. 7.2

Barnes, D. (2015), Antarctic sea ice losses drive gains in benthic carbon drawdown, *Current Biology*, *25*(18), R789–R790, doi:10.1016/j.cub.2015.07.042. 2.1

Bebieva, Y., and K. Speer (2019), The Regulation of Sea Ice Thickness by DoubleDiffusive Processes in the Ross Gyre, *Journal of Geophysical Research: Oceans*, *124*(10), 7068–7081, doi:10.1029/2019JC015247. 2.3.2

Behrenfeld, M. J., and P. G. Falkowski (1997), Photosynthetic rates derived from satellite-based chlorophyll concentration, *Limnology and Oceanography*, *42*(1), 1–20, doi:10.4319/lo.1997.42.1.0001. 7.2

Behrenfeld, M. J., E. Boss, D. A. Siegel, and D. M. Shea (2005), Carbon-based ocean productivity and phytoplankton physiology from space: Phytoplankton growth rates and ocean productivity, *Global Biogeochemical Cycles*, *19*(1), doi:10.1029/2004GB002299. 7.2

Belcher, S. E., A. L. M. Grant, K. E. Hanley, B. Fox-Kemper, L. Van Roekel, P. P. Sullivan, W. G. Large, A. Brown, A. Hines, D. Calvert, A. Rutgersson, H. Pettersson, J.-R. Bidlot, P. A. E. M. Janssen, and J. A. Polton (2012), A global perspective on Langmuir turbulence in the ocean surface boundary layer, *Geophysical Research Letters*, *39*(18), doi:10.1029/2012GL052932. 2.3.2, 8.3

Biddle, L. C., and S. Swart (2020), The Observed Seasonal Cycle of Submesoscale Processes in the Antarctic Marginal Ice Zone, *Journal of Geophysical Research: Oceans*, *125*(6), doi:10.1029/2019JC015587. 2.1, 2.2, 2.3.1, 5.1

Blumen, W. (1978), Uniform Potential Vorticity Flow: Part I. Theory of Wave Interactions and Two-Dimensional Turbulence, *Journal of Atmospheric Sciences*, *35*(5), 774 – 783, doi:10.1175/1520-0469(1978)035<0774:UPVFPI>2.0.CO;2. 8.3

Boccaletti, G., R. Ferrari, and B. Fox-Kemper (2007), Mixed Layer Instabilities and Restratification, *Journal of Physical Oceanography*, *37*(9), 2228–2250, doi:10.1175/JPO3101.1. 2.3.1

Bouffard, D., and L. Boegman (2013), A diapycnal diffusivity model for stratified environmental flows, *Dynamics of Atmospheres and Oceans*, *61-62*, 14–34, doi:10.1016/j.dynatmoce.2013.02.002. 8.3

Boyd, J. P. (1992), The Energy Spectrum of Fronts: Time Evolution of Shocks in Burgers Equation, *Journal of Atmospheric Sciences*, *49*(2), 128 – 139, doi:10.1175/1520-0469(1992)049<0128:TESOFT>2.0.CO;2. 8.3

Boyd, P. W., H. Claustre, M. Levy, D. A. Siegel, and T. Weber (2019), Multi-faceted particle pumps drive carbon sequestration in the ocean, *Nature*, *568*(7752), 327–335, doi:10.1038/s41586-019-1098-2. 2.4

Brenner, S., L. Rainville, J. Thomson, and C. Lee (2020), The evolution of a shallow front in the Arctic marginal ice zone, *Elem Sci Anth*, *8*(1), 17, doi:10.1525/elementa.413. 5.1, 8.2

Briggs, N., M. J. Perry, I. Cetini, C. Lee, E. D'Asaro, A. M. Gray, and E. Rehm (2011), High-resolution observations of aggregate flux during a sub-polar North Atlantic spring bloom, *Deep Sea Research Part I: Oceanographic Research Papers*, *58*(10), 1031–1039, doi:10.1016/j.dsr.2011.07.007. 7.2, 8.3

Browning, T. J., E. P. Achterberg, A. Engel, and E. Mawji (2021), Manganese co-limitation of phytoplankton growth and major nutrient drawdown in the Southern Ocean, *Nature Communications*, *12*(1), 884, doi:10.1038/s41467-021-21122-6. 8.3

Buesseler, K. O. (1998), The decoupling of production and particulate export in the surface ocean, *Global Biogeochemical Cycles*, *12*(2), 297–310, doi:10.1029/97GB03366. 7.2

Callies, J., and R. Ferrari (2013), Interpreting Energy and Tracer Spectra of Upper-Ocean Turbulence in the Submesoscale Range (1200 km), *Journal of Physical Oceanography*, *43*(11), 2456–2474, doi:10.1175/JPO-D-13-063.1. 8.3

Capet, X., J. C. McWilliams, M. J. Molemaker, and A. F. Shchepetkin (2008), Mesoscale to Submesoscale Transition in the California Current System. Part II: Frontal Processes, *Journal of Physical Oceanography*, *38*(1), 44–64, doi:10.1175/2007JPO3672.1. 8.3

Cavan, E. L., F. A. C. Le Moigne, A. J. Poulton, G. A. Tarling, P. Ward, C. J. Daniels, G. M. Fragoso, and R. J. Sanders (2015), Attenuation of particulate organic carbon flux in the Scotia Sea, Southern Ocean, is controlled by zooplankton fecal pellets, *Geophysical Research Letters*, *42*(3), 821–830, doi:10.1002/2014GL062744. 7.3

Cavan, E. L., S. L. C. Giering, G. A. Wolff, M. Trimmer, and R. Sanders (2018), Alternative Particle Formation Pathways in the Eastern Tropical North Pacific's Biological Carbon Pump, *Journal of Geophysical Research: Biogeosciences*, *123*(7), 2198–2211, doi:10.1029/2018JG004392. 7.3

Cetini, I., M. J. Perry, E. D'Asaro, N. Briggs, N. Poulton, M. E. Sieracki, and C. M. Lee (2015), A simple optical index shows spatial and temporal heterogeneity in phytoplankton community composition during the 2008 North Atlantic Bloom Experiment, *Biogeosciences*, *12*(7), 2179–2194, doi:10.5194/bg-12-2179-2015. 7.3

Charney, J. G. (1971), Geostrophic Turbulence, *Journal of the Atmospheric Sciences*, *28*(6), 1087–1095, doi:10.1175/1520-0469(1971)028<1087:GT>2.0.CO;2. 2.3, 8.3

Chelton, D. B., R. A. deSzoeke, M. G. Schlax, K. El Naggar, and N. Siwertz (1998), Geographical Variability of the First Baroclinic Rossby Radius of Deformation, *Journal of Physical Oceanography*, *28*(3), 433–460, doi:10.1175/1520-0485(1998)028<0433:GVOTFB>2.0.CO;2. 5.1

Collen, L. (2005), *Boy*, Bloomsbury., London.

Comiso, J. C., R. A. Gersten, L. V. Stock, J. Turner, G. J. Perez, and K. Cho (2017), Positive Trend in the Antarctic Sea Ice Cover and Associated Changes in Surface Temperature, *Journal of Climate*, *30*(6), 2251–2267, doi:10.1175/JCLI-D-16-0408.1. 2.1

D'Asaro, E., C. Lee, L. Rainville, R. Harcourt, and L. Thomas (2011), Enhanced Turbulence and Energy Dissipation at Ocean Fronts, *Science*, *332*(6027), 318, doi:10.1126/science.1201515. 2.3.1

De Vries, T., and F. Primeau (2011), Dynamically and Observationally Constrained Estimates of Water-Mass Distributions and Ages in the Global Ocean, *Journal of Physical Oceanography*, *41*(12), 2381–2401, doi:10.1175/JPO-D-10-05011.1. (document)

De Vries, T., M. Holzer, and F. Primeau (2017), Recent increase in oceanic carbon uptake driven by weaker upper-ocean overturning, *Nature*, *542*(7640), 215–218, doi:10.1038/nature21068. 1

Deppeler, S. L., and A. T. Davidson (2017), Southern Ocean Phytoplankton in a Changing Climate, *Frontiers in Marine Science*, *4*, doi:10.3389/fmars.2017.00040. 2.4, 7.1

Dove, L. A., A. F. Thompson, D. Balwada, and A. R. Gray (2021), Observational Evidence of Ventilation Hotspots in the Southern Ocean, *Journal of Geophysical Research: Oceans*, *126*(7), doi:10.1029/2021JC017178. 5.2

du Plessis, M., S. Swart, I. J. Ansorge, A. Mahadevan, and A. F. Thompson (2019), Southern Ocean Seasonal Restratification Delayed by Submesoscale WindFront Interactions, *Journal of Physical Oceanography*, *49*(4), 1035–1053, doi:10.1175/JPO-D-18-0136.1. 2.3.1

du Plessis, M. D., S. Swart, L. C. Biddle, I. S. Giddy, P. M. S. Monteiro, C. J. C. Reason, A. F. Thompson, and S. Nicholson (2022), The DailyResolved Southern Ocean Mixed Layer: Regional Contrasts Assessed Using Glider Observations, *Journal of Geophysical Research: Oceans*, *127*(4), doi:10.1029/2021JC017760. 2.1, 5.2, 6.1, 6.2, 8.2, 8.3

Eayrs, C., D. Holland, D. Francis, T. Wagner, R. Kumar, and X. Li (2019), Understanding the Seasonal Cycle of Antarctic Sea Ice Extent in the Context of Longer-Term Variability, *Reviews of Geophysics*, *57*(3), 1037–1064, doi:10.1029/2018RG000631. 2.1

Esters, L., O. Breivik, S. Landwehr, A. ten Doeschate, G. Sutherland, K. H. Christensen, J.-R. Bidlot, and B. Ward (2018), Turbulence Scaling Comparisons in the Ocean Surface Boundary Layer, *Journal of Geophysical Research: Oceans*, *123*(3), 2172–2191, doi:10.1002/2017JC013525. 8.3

Evans, D. G., J. D. Zika, A. C. Naveira Garabato, and A. J. G. Nurser (2018a), The Cold Transit of Southern Ocean Upwelling, *Geophysical Research Letters*, *45*(24), doi:10.1029/2018GL079986. 2.2, 2.3.2, 6.1, 8.3

Evans, D. G., N. S. Lucas, V. Hemsley, E. FrajkaWilliams, A. C. Naveira Garabato, A. Martin, S. C. Painter, M. E. Inall, and M. R. Palmer (2018b), Annual Cycle of Turbulent Dissipation Estimated from Seagliders, *Geophysical Research Letters*, *45*(19), 10,560–10,569, doi:10.1029/2018GL079966. 8.3

Fer, I., A. K. Peterson, and J. E. Ullgren (2014), Microstructure Measurements from an Underwater Glider in the Turbulent Faroe Bank Channel Overflow, *Journal of Atmospheric and Oceanic Technology*, *31*(5), 1128–1150, doi:10.1175/JTECH-D-13-00221.1. 4.2, 4.4

Fitch, D. T., and J. K. Moore (2007), Wind speed influence on phytoplankton bloom dynamics in the Southern Ocean Marginal Ice Zone, *Journal of Geophysical Research*, *112*(C8), C08,006, doi:10.1029/2006JC004061. 8.2

Fox-Kemper, B., R. Ferrari, and R. Hallberg (2008), Parameterization of Mixed Layer Eddies. Part I: Theory and Diagnosis, *Journal of Physical Oceanography*, *38*(6), 1145–1165, doi:10.1175/2007JPO3792.1. 2.3.1, 5.2

Fox-Kemper, B., A. Adcroft, C. W. Böning, E. P. Chassignet, E. Curchitser, G. Danabasoglu, C. Eden, M. H. England, R. Gerdes, R. J. Greatbatch, S. M. Griffies, R. W. Hallberg, E. Hanert, P. Heimbach, H. T. Hewitt, C. N. Hill, Y. Komuro, S. Legg, J. Le Sommer, S. Masina, S. J. Marsland, S. G. Penny, F. Qiao, T. D. Ringler, A. M. Treguier, H. Tsujino, P. Uotila, and S. G. Yeager (2019), Challenges and Prospects in Ocean Circulation Models, *Frontiers in Marine Science*, *6*, 65, doi:10.3389/fmars.2019.00065. 1

Freilich, M., and A. Mahadevan (2021), Coherent Pathways for Subduction From the Surface Mixed Layer at Ocean Fronts, *Journal of Geophysical Research: Oceans*, *126*(5), doi:10.1029/2020JC017042. 2.3.1, 2.4

Frölicher, T., J. Sarmiento, D. Paynter, J. Dunne, J. Krasting, and M. Winton (2015), Dominance of the Southern Ocean in Anthropogenic Carbon and Heat Uptake in CMIP5 Models, *Journal of Climate*, *28*, 862–886,, doi:10.1175/JCLI-D-14-00117.1. 1

Gordon, A. L. (2012), Circumpolar View of the Southern Ocean from 1962 to 1992, *Oceanography*, *25*(3), 18–23. (document)

Gregg, M., E. D'Asaro, J. Riley, and E. Kunze (2018), Mixing Efficiency in the Ocean, *Annual Review of Marine Science*, *10*(1), 443–473, doi:10.1146/annurev-marine-121916-063643. 8.3

Gregor, L., T. J. Ryan-Keogh, S.-A. Nicholson, M. du Plessis, I. Giddy, and S. Swart (2019), GliderTools: A Python Toolbox for Processing Underwater Glider Data, *Frontiers in Marine Science*, *6*, 738, doi:10.3389/fmars.2019.00738. 4.2.2

Gruber, N., M. Gloor, S. E. Mikaloff Fletcher, S. C. Doney, S. Dutkiewicz, M. J. Follows, M. Gerber, A. R. Jacobson, F. Joos, K. Lindsay, D. Menemenlis, A. Mouchet, S. A. Müller, J. L. Sarmiento, and T. Takahashi (2009), Oceanic sources, sinks, and transport of atmospheric CO2, *Global Biogeochemical Cycles*, *23*(1), doi:https://doi.org/10.1029/2008GB003349. 1

Haumann, F. A., N. Gruber, and M. Münnich (2020), SeaIce Induced Southern Ocean Subsurface Warming and Surface Cooling in a Warming Climate, *AGU Advances*, *1*(2), doi:10.1029/2019AV000132. 2.1, 8.1

Hemsley, V. S., T. J. Smyth, A. P. Martin, E. Frajka-Williams, A. F. Thompson, G. Damerell, and S. C. Painter (2015), Estimating Oceanic Primary Production Using Vertical Irradiance and Chlorophyll Profiles from Ocean Gliders in the North Atlantic, *Environmental Science & Technology*, *49*(19), 11,612–11,621, doi:10.1021/acs.est.5b00608. 7.2

Henson, S., F. Le Moigne, and S. Giering (2019), Drivers of Carbon Export Efficiency in the Global Ocean, *Global Biogeochemical Cycles*, *33*(7), 891–903, doi:https://doi.org/10.1029/2018GB006158, _eprint: https://agupubs.onlinelibrary.wiley.com/-doi/pdf/10.1029/2018GB006158. 2.4, 7.1, 7.2

Henson, S. A., C. Laufkötter, S. Leung, S. L. C. Giering, H. I. Palevsky, and E. L. Cavan (2022), Uncertain response of ocean biological carbon export in a changing world, *Nature Geoscience*, doi:10.1038/s41561-022-00927-0. 2.1, 2.4, 7.1, 7.2, 8.2

Hersbach, H., B. Bell, P. Berrisford, G. Biavati, A. Horányi, J. Muñoz Sabater, J. Nicolas, C. Peubey, R. Rozum, A. Simmons, C. Soci, D. Dee, and J.-N. Thépaut (2018), ERA5 hourly data on single levels from 1979 to present. 4.6

Hofman, R. J. (2017), Sealing, whaling and krill fishing in the Southern Ocean: past and possible future effects on catch regulations, *Polar Record*, *53*(1), 88–99, doi:10.1017/S0032247416000644. (document)

Holland, P. R., and R. Kwok (2012), Wind-driven trends in Antarctic sea-ice drift, *Nature Geoscience*, *5*(12), 872–875, doi:10.1038/ngeo1627. 2.1

Hoppema, M. (2004), Weddell Sea is a globally significant contributor to deep-sea sequestration of natural carbon dioxide, *Deep Sea Research Part I: Oceanographic Research Papers*, *51*(9), 1169 – 1177, doi:https://doi.org/10.1016/j.dsr.2004.02.011. 2.2, 2.4, 7.1, 8.2

Horvat, C., E. Tziperman, and J.-M. Campin (2016), Interaction of sea ice floe size, ocean eddies, and sea ice melting, *Geophysical Research Letters*, *43*(15), 8083–8090, doi:10.1002/2016GL069742. 5.1

Huntemann, M., G. Heygster, L. Kaleschke, T. Krumpen, M. Mäkynen, and M. Drusch (2014), Empirical sea ice thickness retrieval during the freeze-up period from SMOS high incident angle observations, *The Cryosphere*, *8*(2), 439–451, doi:10.5194/tc-8-439-2014. 4.6

Iudicone, D., G. Madec, B. Blanke, and S. Speich (2008), The Role of Southern Ocean Surface Forcings and Mixing in the Global Conveyor, *Journal of Physical Oceanography*, *38*(7), 1377–1400, doi:10.1175/2008JPO3519.1. 2.2

Jaeger, G. S., J. A. MacKinnon, A. J. Lucas, E. Shroyer, J. Nash, A. Tandon, J. T. Farrar, and A. Mahadevan (2020), How Spice is Stirred in the Bay of Bengal, *Journal of Physical Oceanography*, *50*(9), 2669–2688, doi:10.1175/JPO-D-19-0077.1. 8.3

Jenkins, W. J. (1982), Oxygen utilization rates in North Atlantic subtropical gyre and primary production in oligotrophic systems, *Nature*, *300*(5889), 246–248, doi:10.1038/300246a0. 7.2

Kelley, D. E. (1990), Fluxes through diffusive staircases: A new formulation, *Journal of Geophysical Research*, *95*(C3), 3365, doi:10.1029/JC095iC03p03365. 6.2

Kheireddine, M., G. Dall'Olmo, M. Ouhssain, G. Krokos, H. Claustre, C. Schmechtig, A. Poteau, P. Zhan, I. Hoteit, and B. H. Jones (2020), Organic Carbon Export and Loss Rates in the Red Sea, *Global Biogeochemical Cycles*, *34*(10), doi:10.1029/2020GB006650. 7.2

Koenig, Z., I. Fer, E. Kolås, T. O. Fossum, P. Norgren, and M. Ludvigsen (2020), Observations of Turbulence at a NearSurface Temperature Front in the Arctic Ocean, *Journal of Geophysical Research: Oceans*, *125*(4), doi:10.1029/2019JC015526. 5.1

Kolmogorov, A. N. (1941), Dissipation of Energy in Locally Isotropic Turbulence, *Akademiia Nauk SSSR Doklady*, *32*, 16. 2.3

Kraichnan, R. H. (1967), Inertial Ranges in Two-Dimensional Turbulence, *Physics of Fluids*, *10*(7), 1417, doi:10.1063/1.1762301. 2.3

Lampitt, R., B. Boorman, L. Brown, M. Lucas, I. Salter, R. Sanders, K. Saw, S. Seeyave, S. Thomalla, and R. Turnewitsch (2008), Particle export from the euphotic zone: Estimates using a novel drifting sediment trap, 234Th and new production, *Deep Sea Research Part I: Oceanographic Research Papers*, *55*(11), 1484–1502, doi:10.1016/j.dsr.2008.07.002. 7.2

Lavergne, T., A. M. Sørensen, S. Kern, R. Tonboe, D. Notz, S. Aaboe, L. Bell, G. Dybkjær, S. Eastwood, C. Gabarro, G. Heygster, M. A. Killie, M. Brandt Kreiner, J. Lavelle, R. Saldo, S. Sandven, and L. T. Pedersen (2019), Version 2 of the EUMETSAT OSI SAF and ESA CCI sea-ice concentration climate data records, *The Cryosphere*, *13*(1), 49–78, doi:10.5194/tc-13-49-2019. 4.6

Lavery, C. (2019), Antarctica and Africa: Narrating alternate futures, *Polar Record*, *55*(5), 347–350, doi:10.1017/S0032247419000743. (document)

Le Moigne, F. A. C., S. A. Henson, R. J. Sanders, and E. Madsen (2013), Global database of surface ocean particulate organic carbon export fluxes diagnosed from the ²³⁴Th technique, *Earth System Science Data*, *5*(2), 295–304, doi:10.5194/essd-5-295-2013. 7.2

Lenton, A., B. Tilbrook, R. M. Law, D. Bakker, S. C. Doney, N. Gruber, M. Ishii, M. Hoppema, N. S. Lovenduski, R. J. Matear, B. I. McNeil, N. Metzl, S. E. Mikaloff Fletcher, P. M. S. Monteiro, C. Rödenbeck, C. Sweeney, and T. Takahashi (2013), Seaair CO₂ fluxes in the Southern Ocean for the period 19902009, *Biogeosciences*, *10*(6), 4037–4054, doi:10.5194/bg-10-4037-2013. 1

Li, Q., B. G. Reichl, B. FoxKemper, A. J. Adcroft, S. E. Belcher, G. Danabasoglu, A. L. M. Grant, S. M. Griffies, R. Hallberg, T. Hara, R. R. Harcourt, T. Kukulka, W. G. Large, J. C. McWilliams, B. Pearson, P. P. Sullivan, L. Van Roekel, P. Wang, and Z. Zheng (2019), Comparing Ocean Surface Boundary Vertical Mixing Schemes Including Langmuir Turbulence, *Journal of Advances in Modeling Earth Systems*, *11*(11), 3545–3592, doi:10.1029/2019MS001810. 8.3

Li, X., D. M. Holland, E. P. Gerber, and C. Yoo (2014), Impacts of the north and tropical Atlantic Ocean on the Antarctic Peninsula and sea ice, *Nature*, *505*(7484), 538–542, doi:10.1038/nature12945. 2.1

Lopez, P., T. C. O'Reilly, and D. Klimov (2015), Cytometers Set Sail With Sea-Going Mobile Robots, *Marine Technology Society Journal*, *49*(3), 17–26, doi:10.4031/MTSJ.49.3.9. 8.3

Lévy, M., P. J. S. Franks, and K. S. Smith (2018), The role of submesoscale currents in structuring marine ecosystems, *Nature Communications*, *9*(1), 4758, doi:10.1038/s41467-018-07059-3. 2.3.1

MacGilchrist, G. A., A. C. Naveira Garabato, P. J. Brown, L. Jullion, S. Bacon, D. C. E. Bakker, M. Hoppema, M. P. Meredith, and S. Torres-Valdés (2019), Reframing the carbon cycle of the subpolar Southern Ocean, *Science Advances*, *5*(8), eaav6410, doi:10.1126/sciadv.aav6410. 2.2, 2.4, 7.1, 8.2

Mahadevan, A. (2016), The Impact of Submesoscale Physics on Primary Productivity of Plankton, *Annual Review of Marine Science*, *8*(1), 161–184, doi:10.1146/annurev-marine-010814-015912. 2.3

Mahadevan, A., E. DAsaro, C. Lee, and M. J. Perry (2012), Eddy-Driven Stratification Initiates North Atlantic Spring Phytoplankton Blooms, *Science*, *337*(6090), 54–58, doi:10.1126/science.1218740. 2.3.1

Maier-Reimer, E., U. Mikolajewicz, and A. Winguth (1996), Future ocean uptake of CO2: interaction between ocean circulation and biology, *Climate Dynamics*, *12*(10), 711–722. 2.4

Manucharyan, G. E., and A. F. Thompson (2017), Submesoscale Sea Ice-Ocean Interactions in Marginal Ice Zones, *Journal of Geophysical Research: Oceans*, *122*(12), 9455–9475, doi:10.1002/2017JC012895. 2.2, 2.3.1, 5.1

Marshall, J., and K. Speer (2012), Closure of the meridional overturning circulation through Southern Ocean upwelling, *Nature Geoscience*, *5*(3), 171–180, doi:10.1038/ngeo1391. 2.2

Martin, J. H., G. A. Knauer, D. M. Karl, and W. W. Broenkow (1987), VERTEX: carbon cycling in the northeast Pacific, *Deep Sea Research Part A. Oceanographic Research Papers*, *34*(2), 267–285, doi:10.1016/0198-0149(87)90086-0. 2.4

Massom, R. A., and S. E. Stammerjohn (2010), Antarctic sea ice change and variability Physical and ecological implications, *Polar Science*, *4*(2), 149 – 186, doi:https://doi.org/10.1016/j.polar.2010.05.001. 2.1, 2.4

McDougall, T. J., and P. M. Barker (2011), *Getting started with TEOS-10 and the Gibbs Seawater (GSW) Oceanographic Toolbox*, Trevor J McDougall, Battery Point, Tas. 4.5

McPhee, M., and J. Morison (2001), Under-ice Boundary Layer, in *Encyclopedia of Ocean Sciences*, pp. 3071–3078, Elsevier, doi:10.1006/rwos.2001.0146. 2.3.2

McWilliams, J. C. (2016), Submesoscale currents in the ocean, *Proceedings of the Royal Society A: Mathematical, Physical and Engineering Sciences*, *472*(2189), 20160,117, doi:10.1098/rspa.2016.0117. 2.3, 2.3.1

Meehl, G. A., J. M. Arblaster, C. T. Y. Chung, M. M. Holland, A. DuVivier, L. Thompson, D. Yang, and C. M. Bitz (2019), Sustained ocean changes contributed to sudden Antarctic sea ice retreat in late 2016, *Nature Communications*, *10*(1), 14, doi:10.1038/s41467-018-07865-9. 2.1

Meredith, M., M. Sommerkorn, S. Cassotta, C. Derksen, A. Ekaykin, A. Hollowed, G. Kofinas, A. Mackintosh, J. Melbourne-Thomas, M. Muelbert, G. Ottersen, H. Pritchard, and E. Schuur (2019), Polar Regions, in *IPCC Special Report on the Ocean and Cryosphere in a Changing Climate*, pp. 203–320, Cambridge University Press, Cambridge, UK and New York, NY, USA. (document), 1, 1.1

Middleton, L., E. C. Fine, J. A. MacKinnon, M. H. Alford, and J. R. Taylor (2021), Estimating Dissipation Rates Associated With Double Diffusion, *Geophysical Research Letters*, *48*(15), doi:10.1029/2021GL092779. 6.2, 8.3

Moore, J. K., W. Fu, F. Primeau, G. L. Britten, K. Lindsay, M. Long, S. C. Doney, N. Mahowald, F. Hoffman, and J. T. Randerson (2018), Sustained climate warming drives declining marine biological productivity, *Science*, *359*(6380), 1139–1143, doi:10.1126/science.aao6379. (document)

Moreau, S., P. W. Boyd, and P. G. Strutton (2020), Remote assessment of the fate of phytoplankton in the Southern Ocean sea-ice zone, *Nature Communications*, *11*(1), 3108, doi:10.1038/s41467-020-16931-0. 7.2

Muench, R. D., H. J. S. Fernando, and G. R. Stegen (1990), Temperature and Salinity Staircases in the Northwestern Weddell Sea, *Journal of Physical Oceanography*, *20*(2), 295–306, doi:10.1175/1520-0485(1990)020<0295:TASSIT>2.0.CO;2. 2.3.2

Nasmyth, P. W. (1970), *Oceanic turbulence*, University of British Columbia, publisher:. 4.4

Naveira Garabato, A. C., G. A. MacGilchrist, P. J. Brown, D. G. Evans, A. J. S. Meijers, and J. D. Zika (2017), High-latitude ocean ventilation and its role in Earth's climate transitions, *Philosophical Transactions of the Royal Society A: Mathematical, Physical and Engineering Sciences*, *375*(2102), 20160,324, doi:10.1098/rsta.2016.0324. 2.4

Nicholson, S.-A., M. Lévy, J. Jouanno, X. Capet, S. Swart, and P. M. S. Monteiro (2019), Iron Supply Pathways Between the Surface and Subsurface Waters of the Southern Ocean: From Winter Entrainment to Summer Storms, *Geophysical Research Letters*, *46*(24), 14,567–14,575, doi:10.1029/2019GL084657. 2.3.2

Nicholson, S.-A., D. B. Whitt, I. Fer, M. D. du Plessis, A. D. Lebéhot, S. Swart, A. J. Sutton, and P. M. S. Monteiro (2022), Storms drive outgassing of CO2 in the subpolar Southern Ocean, *Nature Communications*, *13*(1), 158, doi:10.1038/s41467-021-27780-w. 2.3.2, 8.3

Omand, M. M., E. A. DAsaro, C. M. Lee, M. J. Perry, N. Briggs, I. Cetini, and A. Mahadevan (2015), Eddy-driven subduction exports particulate organic carbon from the spring bloom, *Science*, *348*(6231), 222, doi:10.1126/science.1260062. 2.4

Orozco-Muñiz, J. P., T. Salgado-Jimenez, and N. A. Rodriguez-Olivares (2020), Underwater Glider Propulsion Systems VBS Part 1: VBS Sizing and Glider Performance Analysis, *Journal of Marine Science and Engineering*, *8*(11), 919, doi:10.3390/jmse8110919. 4.2

Osborn, T. R. (1980), Estimates of the Local Rate of Vertical Diffusion from Dissipation Measurements, *Journal of Physical Oceanography*, *10*(1), 83–89, doi:10.1175/1520-0485(1980)010<0083:EOTLRO>2.0.CO;2. 2.3.2, 8.3

OSI-430-b (2019), Global sea-ice concentration interim climate data record 2016 onwards (v2.0), [Online]. 4.6

OSI-450. (2017), Global sea-ice concentration climate data record 1979-2015 (v2.0), [Online]. 4.6

Parkinson, C. L. (2019), A 40-y record reveals gradual Antarctic sea ice increases followed by decreases at rates far exceeding the rates seen in the Arctic, *Proceedings of the National Academy of Sciences*, *116*(29), 14,414–14,423, doi:10.1073/pnas.1906556116. 2.1, 8.1

Pellichero, V., J.-B. Sallée, S. Schmidtko, F. Roquet, and J.-B. Charrassin (2017), The ocean mixed layer under Southern Ocean sea-ice: Seasonal cycle and forcing, *Journal of Geophysical Research: Oceans*, *122*(2), 1608–1633, doi:10.1002/2016JC011970. 2.2, 8.2

Pellichero, V., J.-B. Sallée, C. C. Chapman, and S. M. Downes (2018), The southern ocean meridional overturning in the sea-ice sector is driven by freshwater fluxes, *Nature Communications*, *9*(1), 1789, doi:10.1038/s41467-018-04101-2. 2.1, 2.2, 8.1, 8.2

Pinkerton, M. H., P. W. Boyd, S. Deppeler, A. Hayward, J. Höfer, and S. Moreau (2021), Evidence for the Impact of Climate Change on Primary Producers in the Southern Ocean, *Frontiers in Ecology and Evolution*, *9*, 592,027, doi:10.3389/fevo.2021.592027. 2.4, 7.1, 7.2, 8.2

Platt, T., and S. Sathyendranath (1993), Estimators of primary production for interpretation of remotely sensed data on ocean color, *Journal of Geophysical Research*, *98*(C8), 14,561, doi:10.1029/93JC01001. 7.2

Powell, J. R., and M. D. Ohman (2012), Use of glider-class acoustic Doppler profilers for estimating zooplankton biomass, *Journal of Plankton Research*, *34*(6), 563–568, doi:10.1093/plankt/fbs023. 8.3

Riihelä, A., R. M. Bright, and K. Anttila (2021), Recent strengthening of snow and ice albedo feedback driven by Antarctic sea-ice loss, *Nature Geoscience*, *14*(11), 832–836, doi:10.1038/s41561-021-00841-x. 2.1

Roach, L. A., J. Dörr, C. R. Holmes, F. Massonnet, E. W. Blockley, D. Notz, T. Rackow, M. N. Raphael, S. P. O'Farrell, D. A. Bailey, and C. M. Bitz (2020), Antarctic Sea Ice Area in CMIP6, *Geophysical Research Letters*, *47*(9), doi:10.1029/2019GL086729. 2.1, 8.2

Roden, N. P., B. Tilbrook, T. W. Trull, P. Virtue, and G. D. Williams (2016), Carbon cycling dynamics in the seasonal sea-ice zone of East Antarctica, *Journal of Geophysical Research: Oceans*, *121*(12), 8749–8769, doi:10.1002/2016JC012008. 1

Rudnick, D. L. (2016), Ocean Research Enabled by Underwater Gliders, *Annual Review of Marine Science*, *8*(1), 519–541, doi:10.1146/annurev-marine-122414-033913. (document)

Sallée, J.-B., E. Shuckburgh, N. Bruneau, A. J. S. Meijers, T. J. Bracegirdle, and Z. Wang (2013), Assessment of Southern Ocean mixed-layer depths in CMIP5 models: Historical bias and forcing response: MIXED-LAYER DEPTHS IN CMIP5 MODELS, *Journal of Geophysical Research: Oceans*, *118*(4), 1845–1862, doi:10.1002/jgrc.20157. 1

Sallée, J.-B., V. Pellichero, C. Akhoudas, E. Pauthenet, L. Vignes, S. Schmidtko, A. N. Garabato, P. Sutherland, and M. Kuusela (2021), Summertime increases in upper-ocean stratification and mixed-layer depth, *Nature*, *591*(7851), 592–598, doi:10.1038/s41586-021-03303-x. 8.3

Sanders, R., L. Brown, S. Henson, and M. Lucas (2005), New production in the Irminger Basin during 2002, *Journal of Marine Systems*, *55*(3-4), 291–310, doi:10.1016/j.jmarsys.2004.09.002. 7.2

Sarmiento, J. L., and N. Gruber (2006), *Ocean biogeochemical dynamics*, Princeton University Press. 2.4

Sarmiento, J. L., N. Gruber, M. A. Brzezinski, and J. P. Dunne (2004), High-latitude controls of thermocline nutrients and low latitude biological productivity, *Nature*, *427*(6969), 56–60, doi:10.1038/nature02127. (document)

Sathyendranath, S., R. Brewin, C. Brockmann, V. Brotas, B. Calton, A. Chuprin, P. Cipollini, A. Couto, J. Dingle, R. Doerffer, C. Donlon, M. Dowell, A. Farman, M. Grant, S. Groom, A. Horseman, T. Jackson, H. Krasemann, S. Lavender, V. Martinez-Vicente, C. Mazeran, F. Mélin, T. Moore, D. Müller, P. Regner, S. Roy, C. Steele, F. Steinmetz, J. Swinton, M. Taberner, A. Thompson, A. Valente, M. Zühlke, V. Brando, H. Feng, G. Feldman, B. Franz, R. Frouin, R. Gould, S. Hooker, M. Kahru, S. Kratzer, B. Mitchell, F. Muller-Karger, H. Sosik, K. Voss, J. Werdell, and T. Platt (2019), An Ocean-Colour Time Series for Use in Climate Studies: The Experience of the Ocean-Colour Climate Change Initiative (OC-CCI), *Sensors*, *19*(19), 4285, doi:10.3390/s19194285. 4.6

Scheifele, B., S. Waterman, and J. R. Carpenter (2021), Turbulence and Mixing in the Arctic Oceans Amundsen Gulf, *Journal of Physical Oceanography*, *51*(1), 169–186, doi:10.1175/JPO-D-20-0057.1. 8.2

Scher, H. D., and E. E. Martin (2006), Timing and Climatic Consequences of the Opening of Drake Passage, *Science*, *312*(5772), 428–430, doi:10.1126/science.1120044. (document)

Shaw, W. J., and T. P. Stanton (2014), Dynamic and Double-Diffusive Instabilities in a Weak Pycnocline. Part I: Observations of Heat Flux and Diffusivity in the Vicinity of Maud Rise, Weddell Sea, *Journal of Physical Oceanography*, *44*(8), 1973–1991, doi: 10.1175/JPO-D-13-042.1. 2.3.2

Siegelman, L., P. Klein, P. Rivière, A. F. Thompson, H. S. Torres, M. Flexas, and D. Menemenlis (2020), Enhanced upward heat transport at deep submesoscale ocean fronts, *Nature Geoscience*, *13*(1), 50–55, doi:10.1038/s41561-019-0489-1. 2.4

Small, R. J., A. K. DuVivier, D. B. Whitt, M. C. Long, I. Grooms, and W. G. Large (2021), On the control of subantarctic stratification by the ocean circulation, *Climate Dynamics*, *56*(1-2), 299–327, doi:10.1007/s00382-020-05473-2. 1

Speer, K., S. R. Rintoul, and B. Sloyan (2000), The Diabatic Deacon Cell*, *Journal of Physical Oceanography*, *30*(12), 3212–3222, doi:10.1175/1520-0485(2000)030<3212:TDDC>2.0.CO;2. 2.2

Spreen, G., L. Kaleschke, and G. Heygster (2008), Sea ice remote sensing using AMSR-E 89-GHz channels, *Journal of Geophysical Research: Oceans*, *113*, doi:10.1029/2005JC003384. 4.1

St. Laurent, L., and R. W. Schmitt (1999), The Contribution of Salt Fingers to Vertical Mixing in the North Atlantic Tracer Release Experiment*, *Journal of Physical Oceanography*, *29*(7), 1404–1424, doi:10.1175/1520-0485(1999)029<1404:TCOSFT>2.0.CO;2. 8.3

Stommel, H. (1989), The Slocum Mission, *Oceanography*, *2*(1), 22–25, publisher: Oceanography Society. 4.2.2, 8.3

Su, Z., J. Wang, P. Klein, A. F. Thompson, and D. Menemenlis (2018), Ocean submesoscales as a key component of the global heat budget, *Nature Communications*, *9*(1), 775, doi: 10.1038/s41467-018-02983-w. 2.3.1

Swart, S., S. T. Gille, B. Delille, S. Josey, M. Mazloff, L. Newman, A. F. Thompson, J. Thomson, B. Ward, M. D. du Plessis, E. C. Kent, J. Girton, L. Gregor, P. Heil, P. Hyder, L. P. Pezzi, R. B. de Souza, V. Tamsitt, R. A. Weller, and C. J. Zappa (2019), Constraining Southern Ocean Air-Sea-Ice Fluxes Through Enhanced Observations, *Frontiers in Marine Science*, *6*, 421, doi:10.3389/fmars.2019.00421. 1

Swart, S., M. D. Plessis, A. F. Thompson, L. C. Biddle, I. Giddy, T. Linders, M. Mohrmann, and S. Nicholson (2020), Submesoscale Fronts in the Antarctic Marginal Ice Zone and Their Response to Wind Forcing, *Geophysical Research Letters*, *47*(6), doi:10.1029/2019GL086649. 2.2

Tagliabue, A., J.-B. Sallée, A. R. Bowie, M. Lévy, S. Swart, and P. W. Boyd (2014), Surface-water iron supplies in the Southern Ocean sustained by deep winter mixing, *Nature Geoscience*, *7*(4), 314–320, doi:10.1038/ngeo2101. 2.4

Tagliabue, A., L. Kwiatkowski, L. Bopp, M. Butenschön, W. Cheung, M. Lengaigne, and J. Vialard (2021), Persistent Uncertainties in Ocean Net Primary Production Climate Change

Projections at Regional Scales Raise Challenges for Assessing Impacts on Ecosystem Services, *Frontiers in Climate*, *3*, 738,224, doi:10.3389/fclim.2021.738224. 2.1, 2.4, 8.2

Tamsitt, V., R. P. Abernathey, M. R. Mazloff, J. Wang, and L. D. Talley (2018), Transformation of Deep Water Masses Along Lagrangian Upwelling Pathways in the Southern Ocean, *Journal of Geophysical Research: Oceans*, *123*(3), 1994–2017, doi:10.1002/2017JC013409. 2.2

Thomalla, S. J., N. Fauchereau, S. Swart, and P. M. S. Monteiro (2011), Regional scale characteristics of the seasonal cycle of chlorophyll in the Southern Ocean, *Biogeosciences*, *8*(10), 2849–2866, doi:10.5194/bg-8-2849-2011. 2.4, 7.1

Thomas, L. N., A. Tandon, and A. Mahadevan (2008), Submesoscale processes and dynamics, in *Geophysical Monograph Series*, vol. 177, edited by M. W. Hecht and H. Hasumi, pp. 17–38, American Geophysical Union, Washington, D. C., doi:10.1029/177GM04. 2.2, 2.3.1

Thompson, A. F., A. Lazar, C. Buckingham, A. C. Naveira Garabato, G. M. Damerell, and K. J. Heywood (2016), Open-Ocean Submesoscale Motions: A Full Seasonal Cycle of Mixed Layer Instabilities from Gliders, *Journal of Physical Oceanography*, *46*(4), 1285–1307, doi:10.1175/JPO-D-15-0170.1. 4.2.2

Timmermans, M.-L., and S. R. Jayne (2016), The Arctic Ocean Spices Up, *Journal of Physical Oceanography*, *46*(4), 1277–1284, doi:10.1175/JPO-D-16-0027.1. 8.2

Timmermans, M.-L., and P. Winsor (2013), Scales of horizontal density structure in the Chukchi Sea surface layer, *Continental Shelf Research*, *52*, 39 – 45, doi:https://doi.org/10.1016/j.csr.2012.10.015. 5.1, 8.2, 8.3

Timmermans, M.-L., S. Cole, and J. Toole (2012), Horizontal Density Structure and Restratification of the Arctic Ocean Surface Layer, *Journal of Physical Oceanography*, *42*(4), 659–668, doi:10.1175/JPO-D-11-0125.1. 8.2

Trull, T. W., S. G. Bray, S. J. Manganini, S. Honjo, and R. François (2001), Moored sediment trap measurements of carbon export in the Subantarctic and Polar Frontal zones of the Southern Ocean, south of Australia, *Journal of Geophysical Research: Oceans*, *106*(C12), 31,489–31,509, doi:10.1029/2000JC000308. 8.3

Tréguer, P., C. Bowler, B. Moriceau, S. Dutkiewicz, M. Gehlen, O. Aumont, L. Bittner, R. Dugdale, Z. Finkel, D. Iudicone, O. Jahn, L. Guidi, M. Lasbleiz, K. Leblanc, M. Levy, and P. Pondaven (2018), Influence of diatom diversity on the ocean biological carbon pump, *Nature Geoscience*, *11*(1), 27–37, doi:10.1038/s41561-017-0028-x. 7.3

van der Boog, C. G., H. A. Dijkstra, J. D. Pietrzak, and C. A. Katsman (2021), Double-diffusive mixing makes a small contribution to the global ocean circulation, *Communications Earth & Environment*, *2*(1), 46, doi:10.1038/s43247-021-00113-x. 2.3.2, 8.3

van der Loeff, M. R., P. H. Cai, I. Stimac, A. Bracher, R. Middag, M. B. Klunder, and S. M. van Heuven (2011), 234Th in surface waters: Distribution of particle export flux across the Antarctic Circumpolar Current and in the Weddell Sea during the GEOTRACES expedition ZERO and DRAKE, *Deep Sea Research Part II: Topical Studies in Oceanography*, *58*(25-26), 2749–2766, doi:10.1016/j.dsr2.2011.02.004. 7.2

von Appen, W.-J., C. Wekerle, L. Hehemann, V. Schourup-Kristensen, C. Konrad, and M. H. Iversen (2018), Observations of a Submesoscale Cyclonic Filament in the Marginal Ice Zone, *Geophysical Research Letters*, doi:10.1029/2018GL077897. 5.1

Wenegrat, J. O., L. N. Thomas, M. A. Sundermeyer, J. R. Taylor, E. A. DAsaro, J. M. Klymak, R. K. Shearman, and C. M. Lee (2020), Enhanced mixing across the gyre boundary at the Gulf Stream front, *Proceedings of the National Academy of Sciences*, *117*(30), 17,607–17,614, doi:10.1073/pnas.2005558117. 5.2

Westberry, T., M. J. Behrenfeld, D. A. Siegel, and E. Boss (2008), Carbon-based primary productivity modeling with vertically resolved photoacclimation:Carbon-based Porduction Model, *Global Biogeochemical Cycles*, *22*(2), doi:10.1029/2007GB003078. 7.2

Whitt, D. B., and J. R. Taylor (2017), Energetic Submesoscales Maintain Strong Mixed Layer Stratification during an Autumn Storm, *Journal of Physical Oceanography*, *47*(10), 2419–2427, doi:10.1175/JPO-D-17-0130.1. 8.3

Whitt, D. B., M. Lévy, and J. R. Taylor (2019), Submesoscales Enhance StormDriven Vertical Mixing of Nutrients: Insights From a Biogeochemical Large Eddy Simulation, *Journal of Geophysical Research: Oceans*, *124*(11), 8140–8165, doi:10.1029/2019JC015370. 8.3

Wilson, E. A., S. C. Riser, E. C. Campbell, and A. P. S. Wong (2019), Winter Upper-Ocean Stability and IceOcean Feedbacks in the Sea IceCovered Southern Ocean, *Journal of Physical Oceanography*, *49*(4), 1099–1117, doi:10.1175/JPO-D-18-0184.1. 2.1, 2.3.2

Young, I. R., and A. Ribal (2019), Multiplatform evaluation of global trends in wind speed and wave height, *Science*, *364*(6440), 548–552, doi:10.1126/science.aav9527. 8.2, 8.3

Chapter 9

Scientific papers

An agreement between the University of Gothenburg and the respective Journals allows us to reprint the respective papers in the printed version of this thesis. The reader is referred to the paper titles below:

I: Swart, S., M. du Plessis, A.F. Thompson, L. Biddle, **I. Giddy**, T. Linders, M. Mohrmann, S-A. Nicholson, 2020. Submesoscale Fronts in the Antarctic Marginal Ice Zone and Their Response to Wind Forcing. *Geophysical Research Letters*, **47 (6), e2019GL086649**. https://-doi.org/10.1029/2019GL086649

II: **Giddy, I.**, S. Swart, M. du Plessis, A.F. Thompson, S-A Nicholson. (2021). Stirring of Sea-Ice Meltwater Enhances Submesoscale Fronts in the Southern Ocean. *Journal of Geophysical Research: Oceans*, **126(4), e2020JC016814**. https://doi.org/10.1029/2020JC016814

III: **Giddy, I.**, I. Fer, S. Swart, S-A Nicholson. (*manuscript*, 2022). Vertical convergence of turbulent and double diffusive heat flux drives warming and erosion of Antarctic Winter Water in summer. *in prep for submission to Journal of Physical Oceanography*

IV: **Giddy, I.**, S-A Nicholson, B. Y. Queste, S. Thomalla, S. Swart. (*in review*, 2022). Sea-ice impacts inter-annual variability in phytoplankton phenology and carbon export in the Weddell Sea. *Geophysical Research Letters*